

On the Design and Analysis of LLM-Based Algorithms

Yanxi Chen, Yaliang Li, Bolin Ding, Jingren Zhou

{chenyanxi.cyx, yaliang.li, bolin.ding, jingren.zhou}@alibaba-inc.com

Alibaba Group

Abstract

We initiate a formal investigation into the design and analysis of LLM-based algorithms, i.e. algorithms that contain one or multiple calls of large language models (LLMs) as sub-routines and critically rely on the capabilities of LLMs. While LLM-based algorithms, ranging from basic LLM calls with prompt engineering to complicated LLM-powered agent systems and compound AI systems, have achieved remarkable empirical success, the design and optimization of them have mostly relied on heuristics and trial-and-errors, which is largely due to a lack of formal and analytical study for these algorithms. To fill this gap, we start by identifying the computational-graph representation of LLM-based algorithms, the design principle of task decomposition, and some key abstractions, which then facilitate our formal analysis for the accuracy and efficiency of LLM-based algorithms, despite the black-box nature of LLMs. Through extensive analytical and empirical investigation in a series of case studies, we demonstrate that the proposed framework is broadly applicable to a wide range of scenarios and diverse patterns of LLM-based algorithms, such as parallel, hierarchical and recursive task decomposition. Our proposed framework holds promise for advancing LLM-based algorithms, by revealing the reasons behind curious empirical phenomena, guiding the choices of hyperparameters, predicting the empirical performance of algorithms, and inspiring new algorithm design. To promote further study of LLM-based algorithms, we release our source code at https://github.com/modelscope/agentscope/tree/main/examples/paper_llm_based_algorithm.

Contents

1	Introduction	3
2	LLM-based algorithms	4
2.1	Algorithms as computational graphs	5
2.2	Key abstractions	5
2.3	Formal analysis: accuracy and efficiency	7
2.4	Practical considerations	8
3	Case study: parallel decomposition	9
3.1	Notations and analysis	9
3.2	Concrete examples and experiment settings	11
3.3	Example: counting	12
3.4	Example: sorting	16
3.5	Example: retrieval	22
3.6	Example: retrieval-augmented generation	27
3.7	Example: long-text summarization with chunking	29
4	Case study: hierarchical decomposition	31
4.1	Concrete setup	31
4.2	Algorithm	31
4.3	Analysis	34
4.4	Experiments	36
5	Case study: recursive decomposition	40
5.1	Concrete setup	40
5.2	Algorithm	40
5.3	Analysis	41
5.4	Experiments	42
5.5	Proof of Proposition 2	44
6	Related works	45
7	Conclusion and discussion	46

1 Introduction

The rapid advancements of pre-trained large language models (LLMs) in the past few years [BCE⁺23, WTB⁺22, SMK23] have given rise to the new paradigm of algorithmic problem solving by utilizing LLMs as general-purpose solvers and prompting them with task descriptions plus additional inputs that can help enhance their performance [WWS⁺22, KGR⁺22, ZYY24]. Meanwhile, it is also well recognized that even the best LLMs today still exhibit various limitations, such as finite context window sizes and difficulty with complex reasoning. Some of these limitations are fundamental [MS23, PNP24, TTC⁺24, HR24, WDL24, MPS24], and resolving them requires new breakthroughs. Moreover, in resource-constrained scenarios where using the state-of-the-art LLMs is not feasible, one might have to resort to smaller and weaker LLMs for solving complex tasks.

All these have motivated the developments of what we call *LLM-based algorithms*, namely, algorithms that contain one or multiple LLM calls as sub-routines and fundamentally rely on the capabilities of LLMs. In its most basic form, an LLM-based algorithm can be a combination of one or multiple LLM calls and some prompt engineering [YYZ⁺23, BBK⁺23, ZSH⁺23, WWS⁺23]. More advanced examples include LLM-powered agent systems [MDL⁺23, PKB⁺24, XCG⁺23] and compound AI systems [ZKC⁺24] that augment LLMs with additional abilities like tool use and long-term memory, as well as the emerging paradigm of LLM programming [SSC⁺23, KSM⁺24, ZYX⁺24].

LLM-based algorithms, in a similar spirit to neuro-symbolic programming [CEP⁺21, GK23] and learning-augmented algorithms [MV22, LM22], combine the advantages of both LLMs and traditional algorithms. An LLM-based algorithm, designed with human’s intelligence and knowledge of algorithmic problem solving, can exhibit much better controllability and interpretability, stronger performance that is less reliant on delicate prompting or extensive trial-and-errors, and capabilities that far exceed what could possibly be achieved by directly prompting the LLM for a solution.

The rapid developments of LLM-based algorithms naturally raise the question: is it possible to provide any *formal analysis or guarantee* for LLM-based algorithms? This seems like a daunting task at first glance, due to the black-box nature of LLMs. Indeed, in prior works of this field, LLM-based algorithms have been mostly designed in a heuristic manner, and evaluated empirically with limited insights beyond the measurements of a few error or cost metrics on certain benchmarks. In contrast, formal analysis of LLM-based algorithms, if it does exist, can bring various potential benefits, including but not limited to revealing the reasons behind curious empirical phenomena, instructing choices of hyperparameters, predicting the empirical performance of LLM-based algorithms, and even inspiring new algorithm design.

Main contributions. The goal of this work is to initiate a formal investigation into the design and analysis of LLM-based algorithms. Our contributions to filling this gap, and thereby advancing the field of LLM-based algorithms, are summarized as follows.

- In Section 2, we start by formulating LLM-based algorithms as computational graphs consisting of LLM nodes and non-LLM nodes, and identifying the design principle of task decomposition. We further introduce some key abstractions, based on which formal analysis for the accuracy and efficiency of LLM-based algorithms is developed.
- Section 3 provides an in-depth case study for parallel decomposition, a basic pattern of task decomposition and a building block for more sophisticated LLM-based algorithms. After introducing the general formulation and analysis for this pattern, we present our algorithm design and analysis for multiple concrete tasks, which are then validated by extensive numerical experiments. Advanced case studies for hierarchical decomposition and recursive decomposition are provided in Sections 4 and 5 respectively, which further demonstrate how to apply our proposed analytical framework to diverse scenarios and complex patterns of LLM-based algorithms.
- We derive various novel insights from our analytical and empirical study. For example, considering the hyperparameter m that represents the granularity of parallel decomposition, our analysis explains why error and cost metrics of an LLM-based algorithm are monotone in m in certain cases while non-monotone in others, which in turn guides the choices of m for achieving the desired accuracy or efficiency. Our work exemplifies how to leverage the proposed framework for systematic design and analysis of practical LLM-based algorithms, which can potentially inspire future work in this area.

2 LLM-based algorithms

This section introduces a formal framework for the design and analysis of LLM-based algorithms. In the following, we present an overview for the definition, design principle, and analysis of LLM-based algorithms. Further details are provided afterwards.

Definition. Generally speaking, an *LLM-based algorithm* is simply an algorithm that contains one or multiple LLM calls as its key components. Examples of LLM-based algorithms range from one single LLM call, to LLM-powered agent systems or compound AI systems consisting of a mixture of LLM calls and non-LLM programs. One way of formally representing an LLM-based algorithm is using a *computational graph*, which will soon be elaborated in Section 2.1.

Design principle: task decomposition. An LLM-based algorithm might utilize multiple LLM calls and non-LLM programs to handle sub-tasks derived from the original problem, whose outputs together give rise to the final solution of the overall algorithm. This naturally implies the principle of *task decomposition*. Indeed, one key aspect of designing an LLM-based algorithm is to figure out how to decompose the original task into sub-tasks appropriately, so that each of them can be handled by one LLM call or non-LLM program accurately and efficiently, while the performance of the overall algorithm is also guaranteed.

The principle of task decomposition has been widely adopted, either explicitly or implicitly, in prior works on LLM-based algorithms. There are various reasons why task decomposition is beneficial and oftentimes crucial for solving problems with LLMs, some of which are listed below:

- Despite the rapid developments of Transformer-based LLMs, their context windows are still finite, which limits the problem size that one LLM call can handle. For an LLM that have a very large or even (in theory) infinite context window, its accuracy of solving a class of problems, e.g., long-text retrieval or summarization, will typically decay with the size of the problem, in which case task decomposition is still favorable.
- Other classes of problems might have limited problem sizes, but require complex reasoning for solving them correctly. In this case, LLM-based algorithms can benefit substantially from sequential task decomposition such as step-by-step thinking and acting [YZY⁺23], or parallel decomposition like generating multiple reasoning paths and then aggregating them for a better solution [SLC⁺23, WWS⁺23].
- Aside from accuracy, it is possible that better efficiency can be achieved with task decomposition, compared with one single LLM call. For instance, the input problem might be decomposed into multiple independent sub-tasks that can be solved in parallel, while solving the problem with one LLM call via autoregressive decoding, which is inherently sequential, suffers from a larger end-to-end latency.

Despite all these benefits, it is also possible that fine-grained task decomposition can incur higher errors or costs in certain cases. Choosing the appropriate decomposition is crucial for achieving good performance of the overall algorithm, be it a trade-off between accuracy and efficiency or the best of both worlds.

Remark 1. It is worth noting that one single LLM call can also be treated from the perspective of task decomposition, which is a special case of LLM-based algorithms. Thus the analysis proposed in this work still holds for this case.

Analysis: accuracy and efficiency. Given a task and the corresponding LLM-based algorithm with specific configurations, we aim to analyze its performance, namely how accurately and efficiently the algorithm solves the task, akin to analysis for any generic algorithm. Following the principle of task decomposition, this is done by analyzing for each LLM call or non-LLM program first, and then for the overall algorithm. Given that LLMs are regarded as black-box general-purpose problem solvers using natural language as input and output, we find it useful and necessary to leverage certain abstractions, to be introduced in Section 2.2, in order to facilitate formal analysis that will soon be presented in Section 2.3. One practical usage of formal analysis is to predict the performance of an LLM-based algorithm before actually running it, which will in turn help to optimize certain hyperparameters in the configurations or inspire better algorithm design.

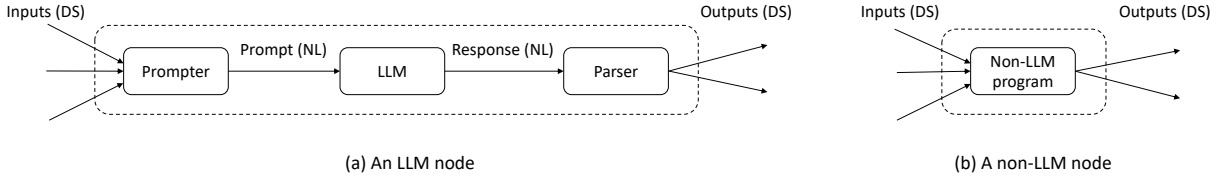


Figure 1: Two types of nodes in the computational graphs of LLM-based algorithms. Each node can have one or multiple inputs/outputs. We use the abbreviation “NL” for “natural language”, and “DS” for “data structure”.

2.1 Algorithms as computational graphs

We formulate an LLM-based algorithm as a computational graph. Each graph node takes some inputs from its predecessor nodes, executes certain operations, and returns some outputs. The nodes can be categorized into two types, which we refer to as *LLM nodes* and *non-LLM nodes*, demonstrated in Figure 1.

- Within an LLM node, the operations consist of a prompter that formats a prompt based on the inputs, an LLM call that processes the prompt, and a parser that extracts the targeted information from the LLM’s response. The prompter and parser, designed for the sub-task of the current node, serve as translators between natural language and traditional data structures. Following the principle of task decomposition, we assume without loss of generality that each LLM node contains one single LLM call.
- Within a non-LLM node, the operations can be anything that does not involve LLMs. Examples include a symbolic algorithm, an API call for a search engine, or a classical machine learning model.

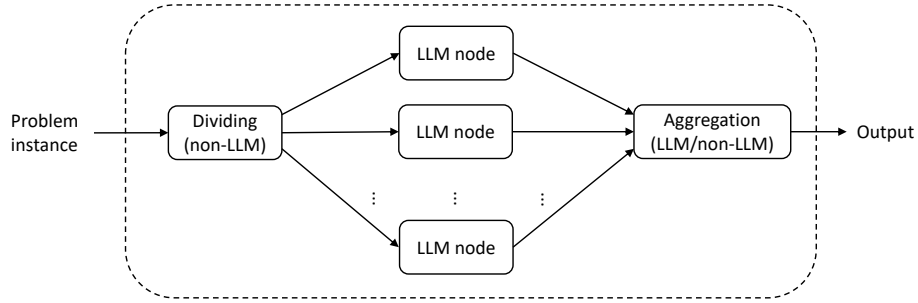
Given such nodes, the computational graph is built by connecting them with directed edges that specify the data flows within the LLM-based algorithm. For example, Figure 2a shows the graph for the pattern of parallel decomposition, which divides the input problem into parallel sub-tasks, solves each of them with one LLM node, and aggregates the results for the final solution; Figure 2b illustrates an algorithm for book-length summarization [CLGI24, Ope24b], which divides the input text into multiple chunks and maintains a global summary via incremental updating; and Figure 2c represents the ReAct algorithm [YZY⁺23], which consists of multiple iterations of reasoning, tool use and aggregation. The computational-graph formulation is expressive enough to cover these diverse LLM-based algorithms that have been proposed separately in prior works, and facilitates formal analysis for all of them in a unified manner. The computational graph of an LLM-based algorithm can be pre-specified and static, or dynamically constructed at runtime, as will be demonstrated later in our case studies in Sections 4 and 5. Configurations of an LLM-based algorithm include how task decomposition is done (reflected by the graph topology and the sub-tasks of graph nodes), the methods of prompting and parsing for each LLM node, configurations of the LLM(s) being used, and so on. The LLM nodes within one graph might use the same or different backbone LLMs.

2.2 Key abstractions

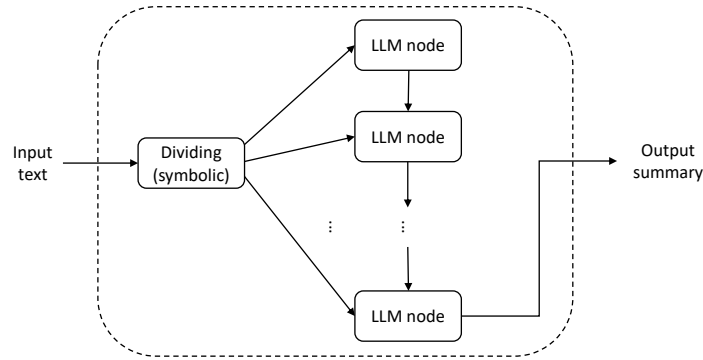
Let us introduce a few key abstractions that facilitate our formal analysis of LLM-based algorithms, namely, how *accurately* and *efficiently* an LLM-based algorithm solve a task. A summary of these abstractions and their relation can be found in Figure 3.

Error and cost metrics. The accuracy and efficiency of each graph node and the overall LLM-based algorithm can be quantified by certain error metrics and cost metrics respectively. The performance of individual graph nodes, together with the graph topology, implies the performance of the overall algorithm. For each specific task or algorithm, one might define multiple error metrics and cost metrics, which can be analyzed in a unified manner within our proposed framework.

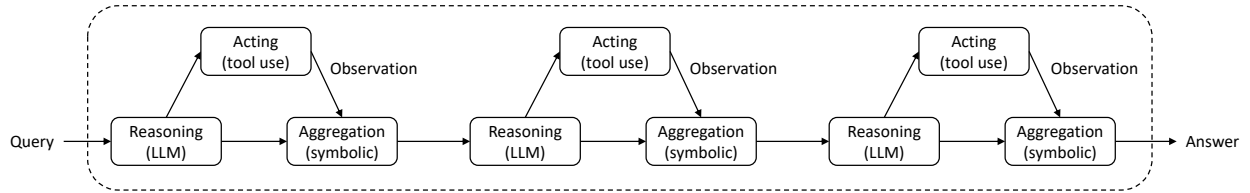
Error metrics are task-specific in general. Moreover, the overall algorithm and the LLM nodes within it might have different error metrics. For instance, consider an LLM-based algorithm that answers a given



(a) Parallel decomposition. See Section 3 for four concrete examples of this pattern.



(b) Book-length summarization, cf. Figure 1 in [CLGI24]. The “dividing” node contains a symbolic program that divides the input text into multiple smaller chunks.



(c) The ReAct algorithm [ZY+23]. Each “acting” node represents one API call for some tool, and each “aggregation” node aggregates the outputs of its predecessor nodes, e.g. by simple concatenation.

Figure 2: Examples of computational-graph representations for LLM-based algorithms.

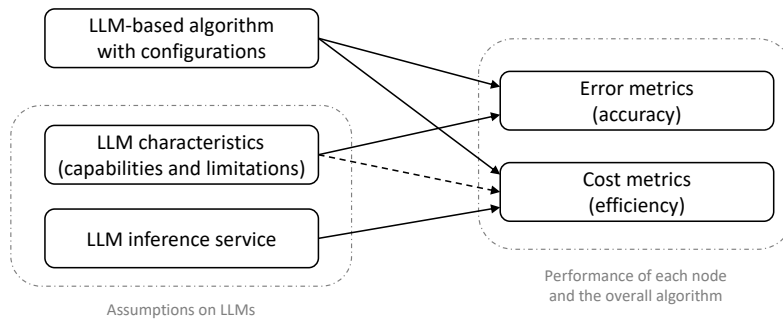


Figure 3: The introduced abstractions and their relation.

question by first retrieving relevant sentences from the input text with multiple LLM nodes, and then reasoning over the extracted sentences with another LLM node. In this case, the overall algorithm is evaluated by whether it answers the question correctly, while each LLM node responsible for retrieval is evaluated by whether it successfully extracts all necessary sentences within the input text that it handles.¹

Cost metrics, on the other hand, are largely task-agnostic. Below are some example cost metrics that might be of interest, regardless of the specific task or algorithm:

- The total length of prompts and total length of generated texts, measured by the numbers of characters or tokens, within one run of the overall algorithm. These metrics are especially relevant to the financial costs when the algorithm uses a proprietary LLM that is accessed via commercial API calls, which are typically charged by the number of tokens. They are also correlated with the time and memory complexities of LLM inference.
- The end-to-end latency of one run of the overall algorithm, namely the time complexity. One particular property of this metric is that the latency can be impacted by parallelism of LLM calls, an important aspect of LLM inference service in practice.
- Other possible cost metrics for one run of an LLM-based algorithm include the peak memory usage, the total number of LLM calls, FLOPs, energy consumption, carbon emission, among others.

Unless specified otherwise, we focus on the costs of the LLM nodes within an LLM-based algorithm, and neglect those of the non-LLM nodes, since the latter is much smaller than the former in all concrete scenarios that we will consider later in this work.

LLM characteristics and inference service. To analyze the error and cost metrics for an LLM-based algorithm, it is necessary to make certain assumptions about the characteristics and inference service of the LLM(s) used within it.

Characteristics of LLMs, namely their *capabilities and limitations*, determine what the generated text will be for a specific prompt, and thus directly affect the error metrics of individual graph nodes and the overall algorithm. They also affect the cost metrics *indirectly*, via the lengths of prompts and generated texts. Assumptions on LLM characteristics can be task-specific or task-agnostic.

Assumptions on LLM inference service [YSZ⁺24, PDC⁺23, ZNH⁺24], on the other hand, are task-agnostic and only affect the cost metrics, not error metrics. In particular, they determine the relation between the cost metrics and the lengths of prompt and generated text for each LLM call, the parallelism of multiple LLM calls, among others. While LLM inference service in practice can be very diverse, we will see in the next subsection that unified and formal analysis is possible with appropriate abstractions of it.

2.3 Formal analysis: accuracy and efficiency

Given the aforementioned formulations and abstractions, we are now ready to consider formal analysis for the accuracy and efficiency of LLM-based algorithms. More specifically, one can first analyze the error and cost metrics for each individual node within the computational graph; these, combined with the graph topology, lead to results about the error and cost metrics of the overall algorithm.

We elaborate this approach in the following. Unless otherwise specified, our analysis is deterministic, for a given task instance and fixed random seed(s).

Analysis of error metrics. The error metrics of the output of each LLM node, which are calculated with respect to what the output should have been if all nodes accomplish their tasks with exact accuracy, depend on the characteristics, i.e. capabilities and limitations, of the LLM, as well as the specific problem instance and random seed(s). For a certain node v , the error of its output y can be bounded by some function f_v (which depends on the aforementioned factors if v is an LLM node) of the errors of its inputs x_1, x_2, \dots, x_k , i.e. the outputs of its predecessor nodes:

$$\mathcal{E}(y) \leq f_v(\mathcal{E}(x_1), \mathcal{E}(x_2), \dots, \mathcal{E}(x_k)). \tag{1}$$

¹Throughout this work, we use “accuracy” to refer to the broader concept of “quality”, and an “error metric” can be any metric that measures how much the output of an algorithm deviates from certain criteria.

The function f_v can be general, with some examples listed in the following:

- $\mathcal{E}(y) \leq \sum_{i \in [k]} \mathcal{E}(x_i)$ or $\frac{1}{k} \sum_{i \in [k]} \mathcal{E}(x_i)$. Such linear relationship can appear in, for example, a simple counting task that will be elaborated in Section 3.3.
- $\mathcal{E}(y) = \min_{i \in [k]} \mathcal{E}(x_i)$. In a task of code generation, the algorithm might generate multiple samples, so that it succeeds as long as one of the samples is correct (e.g. by passing all test cases).
- $\mathcal{E}(y) \leq \max_{i \in [k]} \mathcal{E}(x_i)$. This case can be used for the sorting task to be introduced in Section 3.4, if the node v is responsible for merging multiple sorted lists and \mathcal{E} stands for the ℓ_∞ error.

Finally, the error metrics of the overall algorithm are exactly those of the particular graph node that is responsible for generating the final solution returned by the algorithm.

Analysis of cost metrics. Let us first consider the cost of one LLM call for a specific input prompt, which consists of a *prefilling phase* with a prompt of length \mathcal{L}_{pre} , and a *decoding phase* that generates text of length \mathcal{L}_{dec} . In our framework, we assume that the cost \mathcal{C} of one LLM call can be bounded by

$$\mathcal{C} \leq \mathcal{C}(\text{prefilling}) + \mathcal{C}(\text{decoding}) = \mathcal{C}_{\text{pre}}(\mathcal{L}_{\text{pre}}) + \mathcal{C}_{\text{dec}}(\mathcal{L}_{\text{pre}}, \mathcal{L}_{\text{dec}}) =: \mathcal{C}_{\text{LLM}}(\mathcal{L}_{\text{pre}}, \mathcal{L}_{\text{dec}}). \quad (2)$$

The functions \mathcal{C}_{pre} and \mathcal{C}_{dec} are specific to each LLM call, and depend on the choices of cost metrics and LLM inference service. For example:

- Charges of API calls: \mathcal{C}_{pre} and \mathcal{C}_{dec} are linear functions, namely $\mathcal{C}_{\text{pre}}(\mathcal{L}_{\text{pre}}) = c_{\text{pre}} \times \mathcal{L}_{\text{pre}}$, $\mathcal{C}_{\text{dec}}(\mathcal{L}_{\text{pre}}, \mathcal{L}_{\text{dec}}) = c_{\text{dec}} \times \mathcal{L}_{\text{dec}}$, where c_{pre} and c_{dec} are the cost per token for prompting and text generation, respectively.
- Latency: in a memory-bound scenario [AQS⁺23] where \mathcal{L}_{pre} is limited and the latency of memory IO for loading model weights is dominant, we have approximately $\mathcal{C}_{\text{pre}}(\mathcal{L}_{\text{pre}}) = O(1)$ and $\mathcal{C}_{\text{dec}}(\mathcal{L}_{\text{pre}}, \mathcal{L}_{\text{dec}}) = O(\mathcal{L}_{\text{dec}})$; in more general scenarios, \mathcal{C}_{pre} and \mathcal{C}_{dec} might grow linearly or even quadratically (e.g. for Transformers with full attention [VSP⁺17]) with \mathcal{L}_{pre} and \mathcal{L}_{dec} .

Next, we consider the cost of the overall algorithm, which can be written as a function of the cost metrics of all LLM nodes within its computational graph. It might be a simple sum of the costs of all LLM nodes, e.g. for API costs charged by tokens. Or it can be a more complex function, e.g. for the end-to-end latency in the presence of parallelism. As an example, consider k independent LLM calls with latencies $\mathcal{C}_1, \mathcal{C}_2, \dots, \mathcal{C}_k$ and *ideal* parallelism of degree p , i.e. no extra cost is induced by parallelism; then, the k LLM calls can be divided into $g = \lceil k/p \rceil$ sequential groups, where each group of p parallel LLM calls is bottlenecked by the one with the largest latency, and thus the end-to-end latency of the overall algorithm becomes

$$\mathcal{C} = \sum_{j \in [g]} \max \left\{ \mathcal{C}_{(j-1)p+1}, \mathcal{C}_{(j-1)p+2}, \dots, \mathcal{C}_{\min\{jp, k\}} \right\}. \quad (3)$$

2.4 Practical considerations

Let us comment on a few practical considerations about the aforementioned abstractions and analysis.

- Regarding the capabilities and limitations of LLMs in a specific task, the black-box nature of LLMs can make it challenging to analytically and accurately quantify these factors, in which case one might resort to measuring and profiling in practice. On the positive side, it is oftentimes easier to make certain qualitative assumptions. For example, in many tasks of interest, a larger problem instance is harder than a smaller one, and thus incurs larger error metrics of an LLM call. For practical purposes like optimizing certain hyperparameters of an LLM-based algorithm, such weak assumptions might be sufficient already.
- Understanding LLM inference service, especially from a system perspective, is crucial for in-depth analysis of cost metrics. LLM inference service can be diverse in practice: for example, LLMs might run on CPUs in a personal laptop or on a distributed GPU cluster, inference might be compute-bound or memory-bound, the complexity of long-sequence processing and generation might be linear or quadratic, parallelism at various levels (e.g. multiple LLMs deployed on multiple machines, or batch inference with one LLM) might be supported, and so on. Fortunately, all these are covered by our proposed framework in a unified manner.

3 Case study: parallel decomposition

This section focuses on *parallel decomposition*, a basic MapReduce-like [DG08] pattern visualized in Figure 2a. An algorithm of this pattern first divides the input problem into multiple independent sub-tasks, solves each of them with one LLM node, and finally aggregates the results with an LLM or non-LLM node for the final solution. The intermediate sub-tasks can be solved sequentially or in parallel, which has impacts on certain cost metrics of the overall algorithm. This basic form of task decomposition can be used as a building block for more sophisticated algorithms. Despite its simplicity, interesting analysis and a wide variety of concrete tasks and algorithms can be derived from this pattern, which are presented in the remaining of this section.

3.1 Notations and analysis

Let us start by defining some formal notations that will be useful in our analysis.

- We denote the size of the input problem instance as n . In our study of LLM-based algorithms, the term “size” here typically means the length, e.g. the number of characters or tokens, of the text that represents the input problem instance; it can also be defined in terms of traditional data structures, such as the length of a list.
- Let k denote the number of parallel sub-tasks after decomposition, and m_i denote the size of the i -th sub-task, where $i \in [k]$. It is assumed that $m_i \leq \bar{m}$ for some maximum value \bar{m} that can fit into the context window of the LLM used in the algorithm. For most of our analysis, we will assume for simplicity that $m_i = m$ for all $i \in [k]$, and that $k = O(n/m)$.
- We denote $p \geq 1$ as the maximum degree of parallelism supported by LLM inference service.
- Finally, let \mathcal{L}_{sys} be an upper bound for the length of the system prompt of each LLM call, which includes everything in the prompt except for the size- n input problem instance. The presence of \mathcal{L}_{sys} , which can be large in practice, is essentially due to the fact that the LLM is used as a general-purpose sub-routine, hence specifying the concrete task for each LLM call constitutes part of the complexity.

These notations are summarized in Table 1 for convenient reference.

For notational convenience, we will often write $f(n) \lesssim g(n)$ in place of $f(n) = O(g(n))$, which means there exists a universal constant $C > 0$ such that $f(n) \leq C \cdot g(n)$ for any positive integer n . In addition, $f(n) \asymp g(n)$ means $f(n) \lesssim g(n)$ and $g(n) \lesssim f(n)$ both hold. To further simplify notation, we will often omit the big-O notation in the input arguments of cost functions \mathcal{C}_{pre} and \mathcal{C}_{dec} ; for example, given a prompt of length $\mathcal{L}_{\text{sys}} + O(n)$, we will write the cost of the prefilling phase as $\mathcal{C}_{\text{pre}}(\mathcal{L}_{\text{sys}} + n)$ rather than $\mathcal{C}_{\text{pre}}(\mathcal{L}_{\text{sys}} + O(n))$.

Analysis of cost metrics. We assume for simplicity that all parallel LLM nodes share the same LLM model and inference service, and thus the same cost functions \mathcal{C}_{pre} and \mathcal{C}_{dec} .

In many cases, the cost of the overall algorithm is a simple sum of the costs of all LLM calls involved. Examples include the financial cost when the LLM APIs are charged by tokens, and the end-to-end latency when all LLM calls are executed sequentially. In such cases, we can write the total cost \mathcal{C} as

$$\mathcal{C} = \mathcal{C}(\text{sub-tasks}) + \mathcal{C}(\text{aggregation}),$$

where $\mathcal{C}(\text{aggregation})$ is the cost of the final aggregation step, and

$$\begin{aligned} \mathcal{C}(\text{sub-tasks}) &= k \times \mathcal{C}(\text{one sub-task}) \leq k \times \mathcal{C}_{\text{LLM}}(\mathcal{L}_{\text{sys}} + m, \mathcal{L}_{\text{dec}}) \\ &= k \times \left(\mathcal{C}_{\text{pre}}(\mathcal{L}_{\text{sys}} + m) + \mathcal{C}_{\text{dec}}(\mathcal{L}_{\text{sys}} + m, \mathcal{L}_{\text{dec}}) \right) \\ &\lesssim n \times \frac{\mathcal{C}_{\text{pre}}(\mathcal{L}_{\text{sys}} + m) + \mathcal{C}_{\text{dec}}(\mathcal{L}_{\text{sys}} + m, \mathcal{L}_{\text{dec}})}{m}. \end{aligned} \tag{4}$$

Here, the first inequality follows Eq. (2), the second follows $k \lesssim n/m$, and $\mathcal{L}_{\text{dec}} = \mathcal{L}_{\text{dec}}(m)$ is task-specific, which can be $O(1)$ or $O(m)$ for example.

This basic analysis already provides some hints for tuning the hyperparameter m from the perspective of minimizing costs. Below are a few possible cases, where we assume for simplicity that $\mathcal{L}_{\text{dec}} = O(1)$:

- If $\mathcal{C}_{\text{pre}}(\mathcal{L}_{\text{sys}} + m) + \mathcal{C}_{\text{dec}}(\mathcal{L}_{\text{sys}} + m, 1)$ grows with m at a linear or sub-linear rate, then the right-hand side of Eq. (4) is monotonely decreasing in m , which means $\mathcal{C}(\text{sub-tasks})$ is minimized at $m = \min\{n, \bar{m}\}$.
- It is well known that a Transformer model with full attention suffers from quadratic complexity in long-sequence processing. For this case, a reasonable assumption would be $\mathcal{C}_{\text{pre}}(\mathcal{L}_{\text{sys}} + m) + \mathcal{C}_{\text{dec}}(\mathcal{L}_{\text{sys}} + m, 1) \lesssim (\mathcal{L}_{\text{sys}} + m)^2$, which implies

$$\begin{aligned} \mathcal{C}(\text{sub-tasks}) &\lesssim n \times \frac{\mathcal{C}_{\text{pre}}(\mathcal{L}_{\text{sys}} + m) + \mathcal{C}_{\text{dec}}(\mathcal{L}_{\text{sys}} + m, 1)}{m} \\ &\lesssim n \times \frac{(\mathcal{L}_{\text{sys}} + m)^2}{m} = n \times \left(\frac{\mathcal{L}_{\text{sys}}^2}{m} + m + 2\mathcal{L}_{\text{sys}} \right). \end{aligned}$$

Assuming that \bar{m} is sufficiently large, the right-hand side achieves the minimum $4 \times n \times \mathcal{L}_{\text{sys}}$ at an intermediate value $m = \mathcal{L}_{\text{sys}}$.

- More generally, one may assume that

$$\mathcal{C}_{\text{pre}}(\mathcal{L}_{\text{sys}} + m) + \mathcal{C}_{\text{dec}}(\mathcal{L}_{\text{sys}} + m, 1) \leq \alpha \times (\mathcal{L}_{\text{sys}} + m)^2 + \beta \times (\mathcal{L}_{\text{sys}} + m) + \gamma,$$

which takes into account a more precise characterization of the FLOPs as well as memory IO for loading model weights and KV caches [AQS+23]. In this case, we have

$$\begin{aligned} \mathcal{C}(\text{sub-tasks}) &\lesssim n \times \frac{\mathcal{C}_{\text{pre}}(\mathcal{L}_{\text{sys}} + m) + \mathcal{C}_{\text{dec}}(\mathcal{L}_{\text{sys}} + m, 1)}{m} \\ &\leq n \times \frac{\alpha \times (\mathcal{L}_{\text{sys}} + m)^2 + \beta \times (\mathcal{L}_{\text{sys}} + m) + \gamma}{m} \\ &= n \times \left(\alpha \times m + \frac{\alpha \times \mathcal{L}_{\text{sys}}^2 + \beta \times \mathcal{L}_{\text{sys}} + \gamma}{m} + 2 \times \alpha \times \mathcal{L}_{\text{sys}} + \beta \right), \end{aligned}$$

and the right-hand side is minimized at $m = \sqrt{\mathcal{L}_{\text{sys}}^2 + \mathcal{L}_{\text{sys}} \times \beta/\alpha + \gamma/\alpha}$.

The above analysis can be extended to the case with parallelism, which is especially relevant to the end-to-end latency of the overall algorithm. Considering parallel LLM calls for homogeneous sub-tasks in an ideal setting where parallelism incurs no additional cost, we have $\mathcal{C} = \mathcal{C}(\text{sub-tasks}) + \mathcal{C}(\text{aggregation})$, where

$$\mathcal{C}(\text{sub-tasks}) \leq \left\lceil \frac{k}{p} \right\rceil \times \left(\mathcal{C}_{\text{pre}}(\mathcal{L}_{\text{sys}} + m) + \mathcal{C}_{\text{dec}}(\mathcal{L}_{\text{sys}} + m, \mathcal{L}_{\text{dec}}) \right) \quad (5)$$

according to Eq. (3). For large m such that $k \leq p$, we have $\lceil k/p \rceil = 1$, and thus $\mathcal{C}(\text{sub-tasks}) \leq \mathcal{C}_{\text{pre}}(\mathcal{L}_{\text{sys}} + m) + \mathcal{C}_{\text{dec}}(\mathcal{L}_{\text{sys}} + m, \mathcal{L}_{\text{dec}})$ is monotonely *increasing* in m . On the other hand, for sufficiently small m and hence large k , we have $\lceil k/p \rceil \approx k/p$, and thus the upper bound for $\mathcal{C}(\text{sub-tasks})$ can be approximated by

$$\begin{aligned} \mathcal{C}(\text{sub-tasks}) &\leq \frac{k}{p} \times \left(\mathcal{C}_{\text{pre}}(\mathcal{L}_{\text{sys}} + m) + \mathcal{C}_{\text{dec}}(\mathcal{L}_{\text{sys}} + m, \mathcal{L}_{\text{dec}}) \right) \\ &\lesssim \frac{n}{p} \times \frac{\mathcal{C}_{\text{pre}}(\mathcal{L}_{\text{sys}} + m) + \mathcal{C}_{\text{dec}}(\mathcal{L}_{\text{sys}} + m, \mathcal{L}_{\text{dec}})}{m}, \end{aligned}$$

which might be monotonely *decreasing* in m if $\mathcal{C}_{\text{pre}}(\mathcal{L}_{\text{sys}} + m) + \mathcal{C}_{\text{dec}}(\mathcal{L}_{\text{sys}} + m, \mathcal{L}_{\text{dec}})$ grows with m at a linear or sub-linear rate. In this case, the overall cost $\mathcal{C}(\text{sub-tasks})$ is minimized by $k \succ p$ and hence $m \asymp n/p$.

One implication of the above analysis is that, the optimal value of m that minimizes costs might depend on the choices of cost metrics and assumptions of LLM inference service, among other factors.

Analysis of error metrics. As explained earlier in Section 2.2, error metrics are mostly task-specific, and thus the analysis of error metrics need to be done in a case-by-case manner. For a given task, error metrics for each homogeneous and parallel sub-task typically increases with the size m , although this is not always the case. Error metrics of the overall algorithm after the final aggregation step also depend on the specific task, the method of aggregation, and choices of metrics. We will soon demonstrate the analysis of error metrics in several concrete examples.

Table 1: A list of notations for analysis of parallel decomposition.

Notation	Definition
n	Size of the input problem instance
m	Size of each parallel sub-task, $m \leq \bar{m}$
k	Number of parallel sub-tasks, $k \lesssim n/m$
p	Maximum degree of parallelism
\mathcal{L}_{sys}	Maximum length of the system prompt

3.2 Concrete examples and experiment settings

The rest of this section is dedicated to the analytical and empirical study of a few specific tasks and their corresponding LLM-based algorithms that follow the pattern of parallel decomposition.

Concrete examples. Tasks that we consider in the rest of this section include counting, sorting, retrieval, retrieval-augmented generation (RAG) and long-text summarization, whose details will soon be explained in their corresponding subsections. For each task, we specify the concrete LLM-based algorithm, analyze its performance in terms of error and cost metrics, and validate our analysis with numerical experiments. Error metrics are task-specific, while cost metrics of interest are common among tasks, including the total prefilling length and decoding length, the total number of LLM calls, and the end-to-end latency with sequential or parallel LLM calls. These concrete examples not only confirm the practical advantages of LLM-based algorithms, but also verify that our analysis can help explain or predict the empirical performance of LLM-based algorithms, reveal the reasons behind some interesting empirical phenomena, and instruct the design of algorithms or choices of hyperparameters, e.g. the sub-task size m .

Remark 2. While the tasks under consideration are motivated by practical scenarios, our study will mostly focus on synthetic task design, like many prior works do. This brings numerous benefits, such as avoiding data contamination, allowing full transparency and control over task configurations, and making the current work as self-contained as possible.

Experiment settings. We use the following LLMs in our experiments, which cover a wide range of LLM characteristics and inference service:

- A Llama-3-8B model [Met24], supported by ollama [oll23] and running on a Macbook Pro with a M2 Pro chip and 16GB memory;
- A Llama-3-70B model [Met24], supported by vLLM [KLZ+23] and running on a server with 4 Nvidia A100-80G GPUs;
- A GPT-4-Turbo model [Ope24a], accessed via API queries.

All of these LLMs are chat models. Each LLM call involved in our algorithms is prompted in a chat format, based on the sub-task that it is responsible for. Interested readers are referred to the source code for the prompts used in our experiments. We use greedy decoding, which is deterministic, in all experiments.

Below are a few more details about our experiments. (1) For ideal parallelism of LLM calls, we consider parallelism degree $p = 4$ and $p = \infty$. Latencies in the presence of parallelism are *simulated* according to Eq. (3). (2) In all experiments, the number of tokens for a piece of text is *estimated* using the same tokenizer, namely the `cl100k_base` encoding of the `tiktoken` package². This simplification has no effect on the major conclusions from our experiment results. (3) Our experiment results include curves of some error metric (in blue) or cost metric (in red) versus the problem size n or sub-task size m . For each curve, we plot the mean and standard deviation of measured metrics from multiple independent trials, i.e. multiple randomly generated task instances.

²https://github.com/openai/openai-cookbook/blob/main/examples/How_to_count_tokens_with_tiktoken.ipynb

3.3 Example: counting

As a warm-up exercise, we consider a simple counting task formulated as follows: given a string of length n consisting of letters and digits, the task is to count the number of digits in it. This can be seen as an abstraction or synthetic version of more generic counting tasks in practice.

3.3.1 Algorithm

Below is an LLM-based algorithm that follows the pattern of parallel decomposition:

1. Divide the input string into k disjoint sub-strings of lengths m_1, m_2, \dots, m_k ;
2. For each $i \in [k]$, let LLM count the number of digits in the i -th sub-string, and return its answer y_i ;
3. The final solution of the algorithm is $y = \sum_{i \in [k]} y_i$.

For each LLM call, we prompt the LLM to generate its answer without intermediate reasoning steps³. Thus it is reasonable to assume, based on the LLM’s capability of instruction following, that the text generated by each LLM call has length $\mathcal{L}_{\text{dec}} = O(1)$ and can be parsed into a count number.

3.3.2 Analysis

Let us assume for notational convenience that $m_i = m$ for all $i \in [k]$, and $k = n/m$ is an integer.

Error metrics. Denote the ground-truth count for the complete string as y^* , and the ground-truth count for the i -th sub-string as y_i^* .

- Let \mathcal{E} represent the absolute counting error, then

$$\mathcal{E}(y) := |y - y^*| = \left| \sum_{i \in [k]} (y_i - y_i^*) \right| \leq \sum_{i \in [k]} |y_i - y_i^*| = \sum_{i \in [k]} \mathcal{E}(y_i).$$

In other words, the overall error is upper bounded by the sum of errors of sub-tasks.

- If we let \mathcal{E} represent the normalized counting error instead, then

$$\mathcal{E}(y) := \frac{|y - y^*|}{n} \leq \frac{1}{n} \sum_{i \in [k]} |y_i - y_i^*| = \frac{1}{k} \sum_{i \in [k]} \frac{|y_i - y_i^*|}{m} = \frac{1}{k} \sum_{i \in [k]} \mathcal{E}(y_i).$$

With this metric, the overall error is upper bounded by the average of errors of sub-tasks.

Cost metrics. Our analysis of cost metrics follows Section 3.1. More specifically, we have $\mathcal{L}_{\text{dec}} = O(1)$ by assumption, and $\mathcal{C}(\text{aggregation}) = 0$ since the final step of the algorithm is done by a non-LLM node.

- Considering the total prefilling length and decoding length as cost metrics, one has

$$\begin{aligned} \mathcal{C}(\text{prefilling}) &\lesssim k \times (\mathcal{L}_{\text{sys}} + m) = \frac{n}{m} \times (\mathcal{L}_{\text{sys}} + m) = n \times \left(\frac{\mathcal{L}_{\text{sys}}}{m} + 1 \right), \\ \mathcal{C}(\text{decoding}) &\lesssim k \times 1 = k = \frac{n}{m}, \end{aligned}$$

both of which are monotonely decreasing in m .

- More generally, the sum of costs of all LLM calls is

$$\begin{aligned} \mathcal{C} = \mathcal{C}(\text{sub-tasks}) &\leq k \times \left(\mathcal{C}_{\text{pre}}(\mathcal{L}_{\text{sys}} + m) + \mathcal{C}_{\text{dec}}(\mathcal{L}_{\text{sys}} + m, 1) \right) \\ &= n \times \frac{\mathcal{C}_{\text{pre}}(\mathcal{L}_{\text{sys}} + m) + \mathcal{C}_{\text{dec}}(\mathcal{L}_{\text{sys}} + m, 1)}{m}. \end{aligned}$$

The optimal choice of m under various conditions has been discussed in Section 3.1.

³On the other hand, step-by-step counting can yield a more accurate answer, but also a significantly higher cost, with $\mathcal{L}_{\text{dec}} = O(m)$ rather than $O(1)$.

- For the end-to-end latency with parallelism degree p , we have

$$\begin{aligned} \mathcal{C} = \mathcal{C}(\text{sub-tasks}) &\leq \left\lceil \frac{k}{p} \right\rceil \times \left(\mathcal{C}_{\text{pre}}(\mathcal{L}_{\text{sys}} + m) + \mathcal{C}_{\text{dec}}(\mathcal{L}_{\text{sys}} + m, 1) \right) \\ &= \left\lceil \frac{n}{p \cdot m} \right\rceil \times \left(\mathcal{C}_{\text{pre}}(\mathcal{L}_{\text{sys}} + m) + \mathcal{C}_{\text{dec}}(\mathcal{L}_{\text{sys}} + m, 1) \right). \end{aligned}$$

Under the assumptions explained in Section 3.1, the minimum is achieved around $k = p$ and $m = n/p$.

3.3.3 Experiments

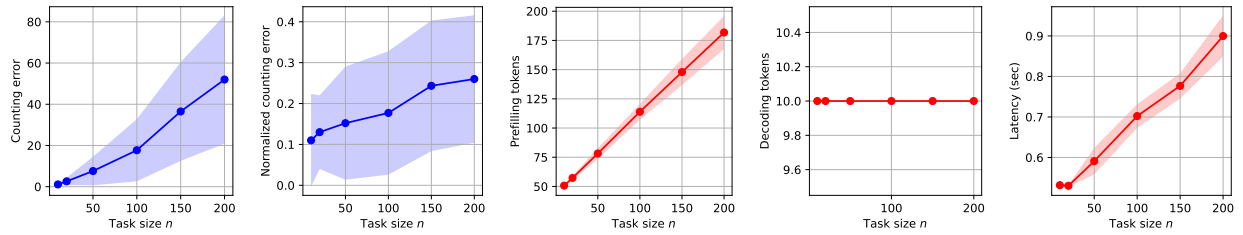
We validate our analysis with numerical experiments. For each problem instance, the input string is generated by randomly sampling n characters from the union of digits, lower-case letters and upper-case letters.

Results with Llama-3-8B. Our empirical results with a Llama-3-8B model are illustrated in Figure 4 and explained in the following.

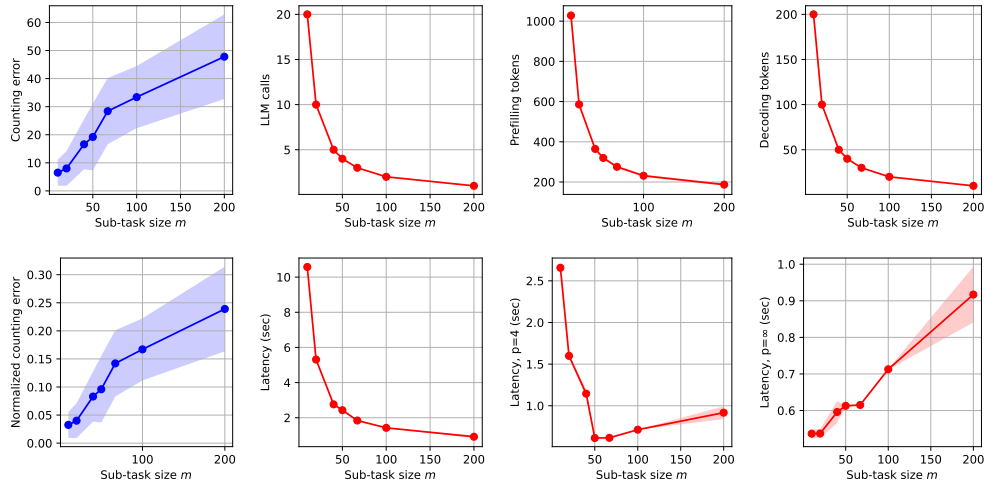
In Figure 4a, we vary the problem size n and set $m = n$ in our algorithm, which means the algorithm becomes equivalent to a single LLM call. Unsurprisingly, error metrics in this counting task monotonely increase with n . The number of prefilling tokens increases linearly with n , while the number of decoding tokens is insensitive to n , since we prompt the LLM to output its answer directly without intermediate reasoning steps. The latency of one LLM call also increases linearly with n , which is likely due to the relatively small sequence lengths and the compute-bound nature of LLM inference by a Llama-3-8B model running on a CPU.

In Figure 4b, we fix $n = 200$ and vary the hyperparameter m , namely the size of each sub-task in our proposed LLM-based algorithm. It is confirmed that decomposing the original task into smaller parallel sub-tasks with a smaller value of m improves the accuracy of the overall algorithm, while incurring higher cost metrics, except for the latency with infinite parallelism (which is monotonely increasing in m) and the latency with parallelism degree $p = 4$ (which achieves the minimum at $m = n/p = 50$, as was predicted by our previous analysis).

Results with GPT-4-Turbo. Figure 5 demonstrates the empirical results for the same experiments but with a GPT-4-Turbo model. We observe from Figure 5a that the latency of one LLM call is insensitive to the input problem size n , which is likely because LLM inference of GPT-4-Turbo is memory-bound for the range of sequence lengths considered in our experiments. One potential implication is that, for the LLM-based algorithm with parallel decomposition, the latency with infinite parallelism $p = \infty$ might slightly increase for smaller m and hence larger k , due to the random variation of latencies in reality; this is indeed what we observe from Figure 5b. Other than that, the results in Figure 5 are similar to those in Figure 4.

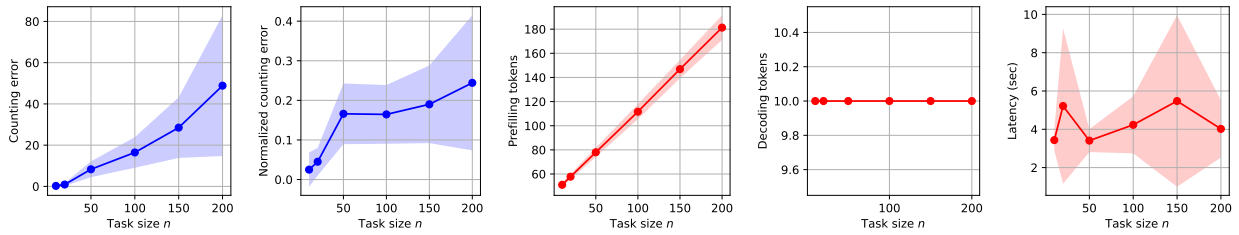


(a) Vary n and set $m = n$. (10 trials)

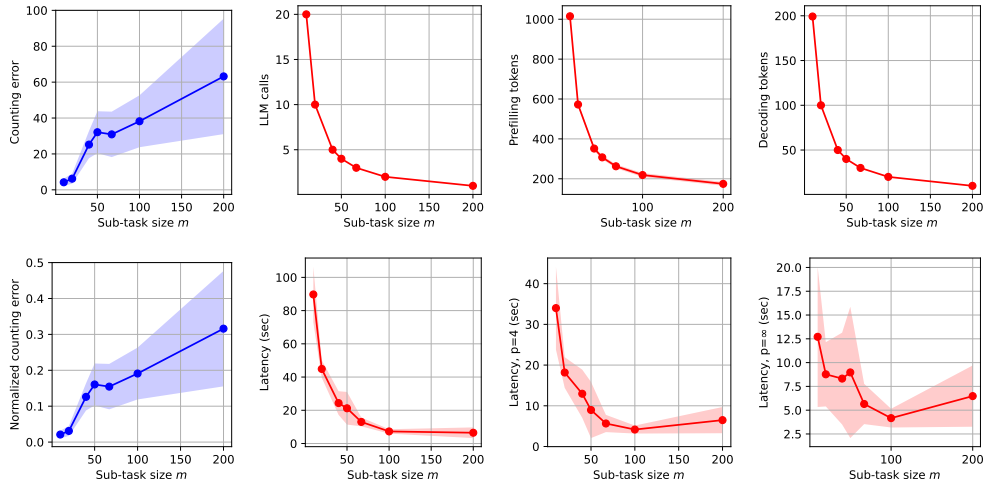


(b) Fix $n = 200$ and vary m . (10 trials)

Figure 4: Empirical results for counting with Llama-3-8B.



(a) Vary n and set $m = n$. (20 trials)



(b) Fix $n = 200$ and vary m . (10 trials)

Figure 5: Empirical results for counting with GPT-4-Turbo.

3.4 Example: sorting

For a more challenging example, let us consider the classical sorting problem: given a list of n numbers $\mathbf{x} \in \mathbb{R}^n$, the task is to sort it in ascending order.

3.4.1 Algorithm

Below is an LLM-based algorithm for sorting a list, which generalizes the naive approach of sorting the list with one single LLM call:

1. Divide the input list \mathbf{x} into k disjoint sub-lists $\mathbf{x}_1, \dots, \mathbf{x}_k$ of lengths m_1, \dots, m_k ;
2. For each $i \in [k]$, use one LLM call to sort the i -th sub-list, which returns a solution \mathbf{y}_i ;
3. Merge the sub-lists $\mathbf{y}_1, \dots, \mathbf{y}_k$ into a single list \mathbf{y} using a symbolic algorithm.

We note two details about this algorithm. (1) To ensure efficiency and stability, for each LLM call, we prompt the LLM to generate the sorted list directly, without intermediate reasoning steps. It has been verified empirically that the LLMs considered in our experiments can follow such instructions, and generate text of length $\mathcal{L}_{\text{dec}}(m) = O(m)$ that can be easily parsed into a list. (2) Step 3 of the algorithm relies on a classical symbolic algorithm for merging two sorted lists, which maintains two moving pointers, one for each list, and chooses each entry of the merged list by comparing the values corresponding to the two pointers. Merging multiple sorted lists can be done by merging one pair of lists at a time, in an incremental or hierarchical manner. Python code for these procedures can be found in Listing 1 at the end of this subsection. Although they are designed under the assumption that the input lists are sorted, they can also be applied to input lists that are not fully sorted, which can possibly happen within the LLM-based algorithm since the input lists in Step 3 are generated by LLM calls in Step 2.

3.4.2 Analysis

Let us assume for notational convenience that $m_i = m$ for all $i \in [k]$, and $k = n/m$ is an integer.

Error metrics. Compared to counting, there are more diverse phenomena in the sorting task in terms of error metrics. In particular, multiple possible failure modes exist in sorting with an LLM-based algorithm:

1. The output list might not be monotone;
2. The length of the output list might be larger or smaller than that of the input list;
3. The output list might contain numbers that do not match exactly those of the input list.

Based on these failure modes, we define the following error metrics for sorting a list, where \mathbf{y} denotes the solution returned by the algorithm and \mathbf{y}^* denotes the ground-truth solution:

- *Exact-match error:* $\mathcal{E} = 0$ if \mathbf{y} matches \mathbf{y}^* exactly, and $\mathcal{E} = 1$ otherwise;
- *Non-monotonicity error:* $\mathcal{E} = \sum_{i \in [n-1]} \max\{y_i - y_{i+1}, 0\}$, which is zero if and only if \mathbf{y} is sorted;
- *Length-mismatch error:* $\mathcal{E} = \frac{1}{n} |\text{len}(\mathbf{y}) - \text{len}(\mathbf{y}^*)| = \frac{1}{n} |\text{len}(\mathbf{y}) - n|$;
- *Fuzzy ℓ_∞ and fuzzy normalized ℓ_1 errors:* we first convert, via simple extending or truncating, the output solution \mathbf{y} to a version $\hat{\mathbf{y}}$ that matches the length n of the input list, and then calculate the fuzzy ℓ_∞ error as $\mathcal{E} = \|\hat{\mathbf{y}} - \mathbf{y}^*\|_\infty = \max_{i \in [n]} |\hat{y}_i - y_i^*|$, or the fuzzy normalized ℓ_1 error as $\mathcal{E} = \frac{1}{n} \|\hat{\mathbf{y}} - \mathbf{y}^*\|_1 = \frac{1}{n} \sum_{i \in [n]} |\hat{y}_i - y_i^*|$.

Note that the same error metrics can be similarly defined for each parallel sub-task in Step 2 of the LLM-based algorithm, and it is reasonable to expect that they become smaller as the sub-task size m decreases. On the other hand, analyzing the error metrics of the overall algorithm after the final merging step can be more complicated, and might be an interesting theoretical problem on its own. As an example, focusing on the third failure mode and the ℓ_∞ error metric, we have the following guarantee, whose proof is deferred after the experiments in this subsection.

Proposition 1. Assume that for each $i \in [k]$, the solution \mathbf{y}_i returned by one LLM call for the i -th sub-task is monotone, matches the length of the corresponding input \mathbf{x}_i , and has an ℓ_∞ error \mathcal{E}_i . Then the ℓ_∞ error of the final solution \mathbf{y} is upper bounded by $\mathcal{E} \leq \max\{\mathcal{E}_1, \dots, \mathcal{E}_k\}$.

Cost metrics. Our analysis of cost metrics for the LLM-based sorting algorithm follows Section 3.1, and is similar to that for counting. One major difference is that $\mathcal{L}_{\text{dec}} = O(m)$ rather than $O(1)$ for each sub-task.

- Considering the total prefilling length and decoding length as cost metrics, one has

$$\begin{aligned} \mathcal{C}(\text{prefilling}) &\lesssim k \times (\mathcal{L}_{\text{sys}} + m) = \frac{n}{m} \times (\mathcal{L}_{\text{sys}} + m) = n \times \left(\frac{\mathcal{L}_{\text{sys}}}{m} + 1\right), \\ \mathcal{C}(\text{decoding}) &\lesssim k \times m = n. \end{aligned}$$

The former is decreasing in m , while the latter is insensitive to m .

- More generally, the sum of costs of all LLM calls is

$$\begin{aligned} \mathcal{C} = \mathcal{C}(\text{sub-tasks}) &\leq k \times \left(\mathcal{C}_{\text{pre}}(\mathcal{L}_{\text{sys}} + m) + \mathcal{C}_{\text{dec}}(\mathcal{L}_{\text{sys}} + m, m)\right) \\ &= n \times \frac{\mathcal{C}_{\text{pre}}(\mathcal{L}_{\text{sys}} + m) + \mathcal{C}_{\text{dec}}(\mathcal{L}_{\text{sys}} + m, m)}{m}. \end{aligned}$$

- For the end-to-end latency with parallelism degree p , we have

$$\begin{aligned} \mathcal{C} = \mathcal{C}(\text{sub-tasks}) &\leq \left\lceil \frac{k}{p} \right\rceil \times \left(\mathcal{C}_{\text{pre}}(\mathcal{L}_{\text{sys}} + m) + \mathcal{C}_{\text{dec}}(\mathcal{L}_{\text{sys}} + m, m)\right) \\ &= \left\lceil \frac{n}{p \cdot m} \right\rceil \times \left(\mathcal{C}_{\text{pre}}(\mathcal{L}_{\text{sys}} + m) + \mathcal{C}_{\text{dec}}(\mathcal{L}_{\text{sys}} + m, m)\right). \end{aligned}$$

3.4.3 Experiments

We validate our analysis with numerical experiments. The input list of each problem instance is generated by randomly sampling entries of the list from the uniform distribution over the interval $[0, 1]$ and then rounding each of them to two decimals.

Results with Llama-3-70B. Our empirical results with a Llama-3-70B model are illustrated in Figure 6 and explained in the following.

In Figure 6a, we vary the problem size n and set $m = n$ in the LLM-based algorithm, in which case the algorithm becomes equivalent to a single LLM call. We make the following observations:

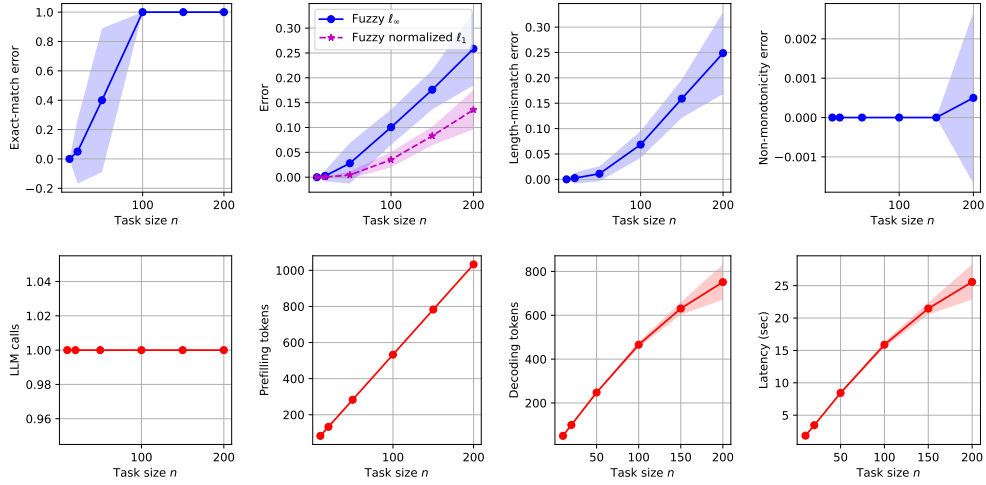
- Unsurprisingly, all error metrics in this task monotonely increase with n .
- While the LLM might output a list that deviates from the ground-truth solution, it is at least good at ensuring that the output list itself is sorted or has a very small non-monotonicity error.
- The prefilling length grows linearly with n , while the growth of the decoding length and end-to-end latency slows down slightly for large values of n , which is mainly because the LLM is prone to returning a list that is shorter than the input list when n is large, as reflected in the length-mismatch error curve.

In Figure 6b, we fix $n = 200$ and vary the sub-task size m . It is confirmed that decomposing the original task into smaller parallel sub-tasks with a smaller value of m implies lower error metrics achieved by the overall algorithm, while increasing certain cost metrics. Two specific observations:

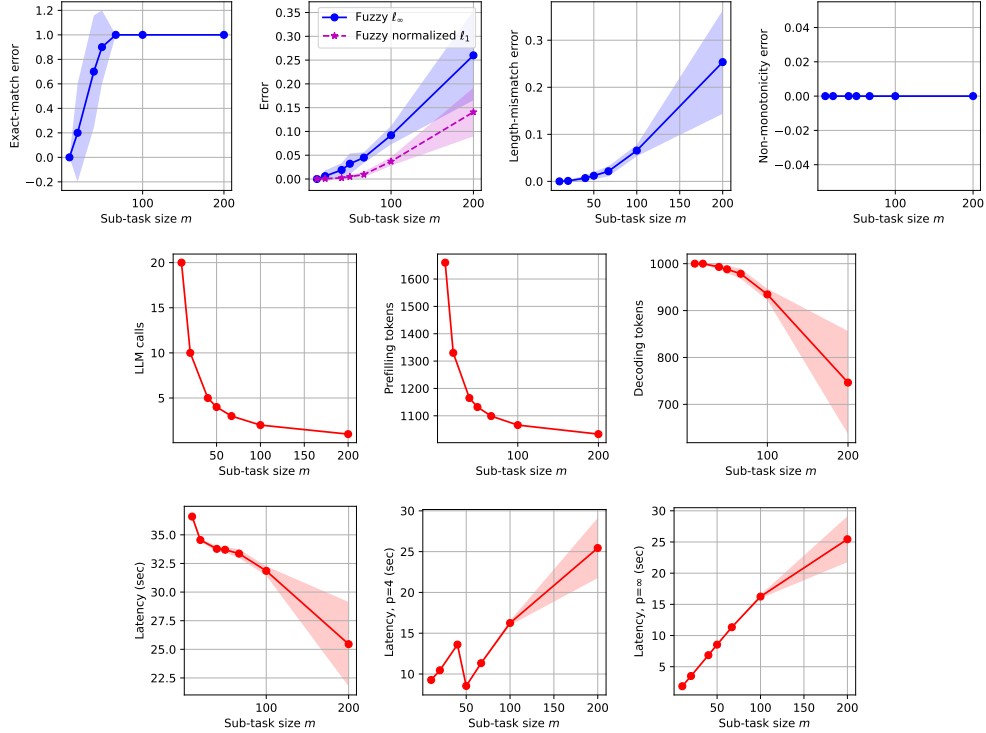
- The total number of decoding tokens decreases with m at a rate that matches the length-mismatch error curve. This does not contradict our previous analysis, which predicts an *upper bound* that is insensitive to the value of m .
- Regarding the end-to-end latency with parallelism degree $p = 4$, the zigzag part of the curve might seem curious. In fact, a fine-grained analysis can well explain this phenomenon. If we approximate the latency for one LLM call solving a sub-task of size m by $O(m)$, then the end-to-end latency of the overall algorithm is approximately $O(m \times \lceil k/p \rceil)$. The numbers calculated in Table 2 for the concrete setting of this experiment match the empirical results and explain the zigzag part.

Table 2: Fine-grained analysis for the latency with parallelism degree $p = 4$ in Figure 6b, where $n = 200$.

Sub-task size m	10	20	40	50	67	100	200
Number of sub-tasks $k = \lceil n/m \rceil$	20	10	5	4	3	2	1
Sequential depth $d = \lceil k/p \rceil$	5	3	2	1	1	1	1
Predicted latency $\asymp d \times m$	50	60	80	50	67	100	200

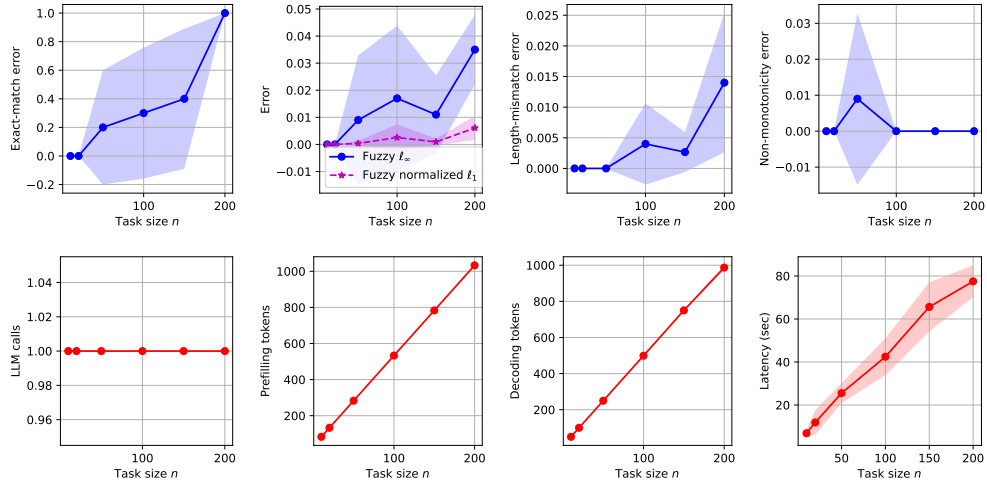


(a) Vary n and set $m = n$. (20 trials)

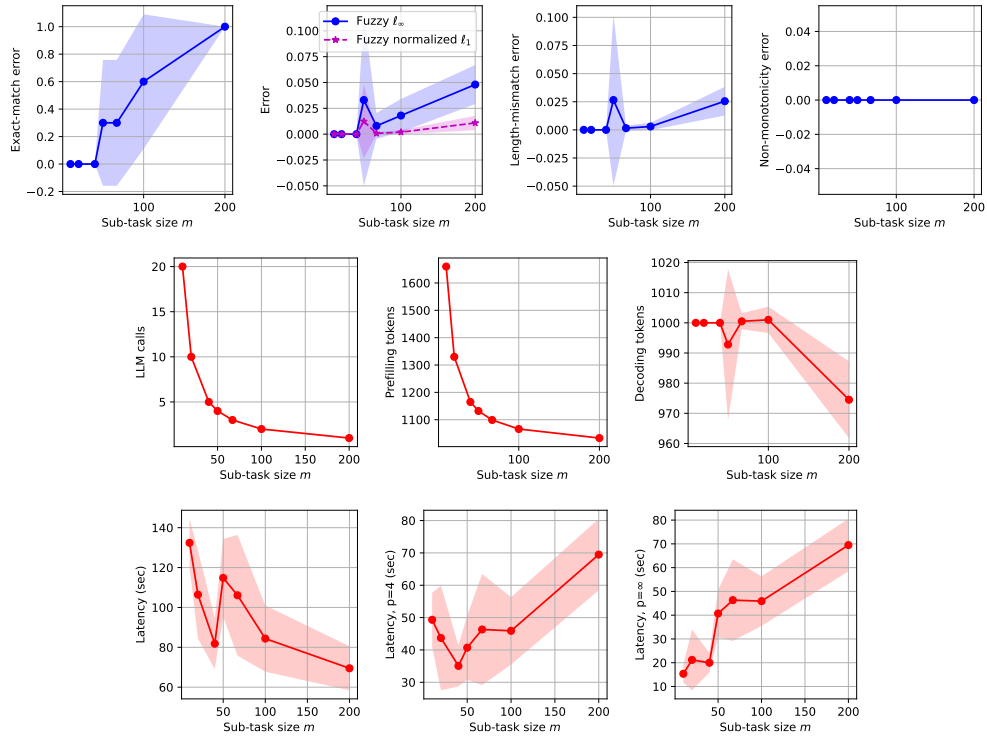


(b) Fix $n = 200$ and vary m . (10 trials)

Figure 6: Empirical results for sorting with Llama-3-70B.



(a) Vary n and set $m = n$. (10 trials)



(b) Fix $n = 200$ and vary m . (10 trials)

Figure 7: Empirical results for sorting with GPT-4-Turbo.

Results with GPT-4-Turbo. Figure 7 demonstrates the empirical results for the same experiments but with a GPT-4-Turbo model. Similar observations can be made from these results, except that latencies exhibit higher variance due to the inference service of GPT-4-Turbo.

3.4.4 Proof of Proposition 1

Recall that \mathbf{y}_i denotes the solution returned by an LLM call, which is assumed to be monotone, for sorting the i -th input sub-list. Let \mathbf{y}_i^* denote the ground-truth solution for sorting the i -th input sub-list. Assuming that $\|\mathbf{y}_i - \mathbf{y}_i^*\|_\infty \leq \epsilon$ for all $i \in [k]$, our goal is to prove that $\|\mathbf{y} - \mathbf{y}^*\|_\infty \leq \epsilon$.

It is easy to check that merging multiple sorted lists is equivalent to sorting the concatenation of the lists. Therefore, we have

$$\begin{aligned}\mathbf{y} &= \text{sort}([\mathbf{y}_1, \dots, \mathbf{y}_k]) = \text{sort}(\text{permute}([\mathbf{y}_1, \dots, \mathbf{y}_k])), \\ \mathbf{y}^* &= \text{sort}([\mathbf{y}_1^*, \dots, \mathbf{y}_k^*]) = \text{sort}(\text{permute}([\mathbf{y}_1^*, \dots, \mathbf{y}_k^*])),\end{aligned}$$

where permute can be any permutation of n elements in a list. In particular, we let permute be the permutation that sorts $[\mathbf{y}_1^*, \dots, \mathbf{y}_k^*]$, which implies

$$\mathbf{y}^* = \text{sort}(\text{permute}([\mathbf{y}_1^*, \dots, \mathbf{y}_k^*])) = \text{permute}([\mathbf{y}_1^*, \dots, \mathbf{y}_k^*]).$$

Also notice that

$$\|\text{permute}([\mathbf{y}_1, \dots, \mathbf{y}_k]) - \text{permute}([\mathbf{y}_1^*, \dots, \mathbf{y}_k^*])\|_\infty = \|[\mathbf{y}_1, \dots, \mathbf{y}_k] - [\mathbf{y}_1^*, \dots, \mathbf{y}_k^*]\|_\infty = \max_{i \in [k]} \|\mathbf{y}_i - \mathbf{y}_i^*\|_\infty \leq \epsilon.$$

Based on the above analysis, our initial goal boils down to the following problem: given two lists $\mathbf{z}, \mathbf{z}^* \in \mathbb{R}^n$ such that $\|\mathbf{z} - \mathbf{z}^*\|_\infty \leq \epsilon$ and \mathbf{z}^* is sorted, we need to show that $\|\text{sort}(\mathbf{z}) - \mathbf{z}^*\|_\infty \leq \epsilon$. Here, \mathbf{z} corresponds to $\text{permute}([\mathbf{y}_1, \dots, \mathbf{y}_k])$, and \mathbf{z}^* corresponds to \mathbf{y}^* .

To prove this, let us consider the classical in-place insertion-sort algorithm illustrated in Algorithm 1. We choose to prove by induction that, throughout the execution of this algorithm, it always holds that $\|\mathbf{z} - \mathbf{z}^*\|_\infty \leq \epsilon$, which immediately implies $\|\text{sort}(\mathbf{z}) - \mathbf{z}^*\|_\infty \leq \epsilon$. To prove this, notice that the only place in Algorithm 1 where \mathbf{z} is changed is the step of swapping z_j and z_{j-1} when the condition $z_j < z_{j-1}$ is satisfied. Under this condition, we have the following:

$$\begin{aligned}z_{j-1} - z_j^* &> z_j - z_j^* &&\geq -\epsilon, \\ z_{j-1} - z_j^* &\leq z_{j-1} - z_{j-1}^* &&\leq \epsilon, \\ z_j - z_{j-1}^* &< z_{j-1} - z_{j-1}^* &&\leq \epsilon, \\ z_j - z_{j-1}^* &\geq z_j - z_j^* &&\geq -\epsilon,\end{aligned}$$

which implies $|z_{j-1} - z_j^*| \leq \epsilon$ and $|z_j - z_{j-1}^*| \leq \epsilon$. This means that the ℓ_∞ error bound is preserved after this swapping step, which concludes our proof.

Algorithm 1: The classical insertion-sort algorithm

- 1 **Input:** a list $\mathbf{z} \in \mathbb{R}^n$ to be sorted.
 - 2 **for** $i = 2, 3, \dots, n$ **do**
 - 3 **for** $j = i, i - 1, \dots, 2$ **do**
 - 4 **if** $z_j \geq z_{j-1}$ **then**
 - 5 Break.
 - 6 Swap z_j and z_{j-1} .
 - 7 **Output:** the sorted list \mathbf{z} .
-

```

1 import numpy as np
2
3
4 def merge_two_sorted_lists(list1, list2):
5     """Merge two non-empty lists or np.arrays that are
6     assumed to be (at least approximately) sorted"""
7
8     len1, len2 = len(list1), len(list2)
9     idx1, idx2 = 0, 0
10    idx = 0
11    solution = np.zeros(len1 + len2)
12    while idx < len1 + len2:
13        if idx1 == len1:
14            val = list2[idx2]
15            idx2 += 1
16        elif idx2 == len2:
17            val = list1[idx1]
18            idx1 += 1
19        else:
20            val1, val2 = list1[idx1], list2[idx2]
21            if val1 <= val2:
22                val = val1
23                idx1 += 1
24            else:
25                val = val2
26                idx2 += 1
27        solution[idx] = val
28        idx += 1
29
30    return solution
31
32
33 def merge_sorted_lists_incremental(lists):
34     """Merge lists = [list1, list2, ...] in an incremental manner"""
35
36     for _ in range(len(lists) - 1):
37         list1 = lists.pop()
38         list2 = lists.pop()
39         solution = merge_two_sorted_lists(list1, list2)
40         lists.append(solution)
41
42     return lists[0]
43
44
45 def merge_sorted_lists_hierarchical(lists):
46     """Merge lists = [list1, list2, ...] in a hierarchical manner"""
47
48     while len(lists) > 1:
49         niters = len(lists) // 2
50         for _ in range(niters):
51             list1 = lists.pop(0)
52             list2 = lists.pop(0)
53             solution = merge_two_sorted_lists(list1, list2)
54             lists.append(solution)
55
56     return lists[0]

```

Listing 1: Python code for merging sorted lists. We choose the hierarchical option in our experiments.

3.5 Example: retrieval

We study a more realistic application of LLM-based algorithms, which is answering a given question that requires retrieving some key information from a long piece of text. Our design of this task draws inspiration from the needle-in-a-haystack benchmark [Kam23] and other similar benchmarks that have been widely adopted for evaluating the long-context capability of LLMs as well as techniques of retrieval-augmented generation [WBC⁺15, Rou23, KBA⁺24, MJ23, ZCH⁺24].

Consider the following setting as an example. A key message (the needle) of the form “The passcode to the {targeted object, e.g. red door} is {6-digit passcode}” is randomly inserted into a piece of long text (the haystack). The algorithm is asked to answer the question “What is the passcode to the {targeted object}?”. To make the problem more challenging and fun, we let the haystack consist of alike sentences of the form “The passcode to the {colored object, e.g. red lock or green door} is {6-digit passcode}”, with colored objects different from the targeted object. This allows us to investigate both sides of retrieval capabilities of LLMs and LLM-based algorithms: retrieving the targeted information correctly, while avoiding being confused or misled by background information that might seem relevant to the question [SCM⁺23].

Note that while we use this concrete setting for our empirical study, the proposed algorithm and analysis in the following are actually applicable to generic settings of this retrieval task.

3.5.1 Algorithm

We consider the following LLM-based algorithm that follows the pattern of parallel decomposition:

1. Divide the input text of length n into k overlapping chunks of lengths m_1, \dots, m_k ;
2. For each chunk, use one LLM call to try to answer the question based on that chunk;
3. Generate the final answer by majority voting.

We note a few details about this algorithm. (1) All lengths involved here are measured by the number of characters. (2) In the first step of chunking, we let each pair of adjacent chunks share an overlap that is larger than the length of the needle, to ensure that the needle will appear as a whole in at least one chunk. (3) For each LLM call in the second step, the LLM is prompted to answer “I don’t know” if it believes that there is not sufficient information in the corresponding chunk, e.g. when the chunk simply does not contain the needle. Such answers will be excluded from the final step of the algorithm. (4) In the final step of majority voting, it is possible that there are multiple (say h) candidate solutions with the same frequency, in which case we let the algorithm return the list of such candidates. If this list contains the ground-truth solution, we calculate the exact-match error as $1 - 1/h$ in our experiments.

3.5.2 Analysis

Let us assume for concreteness that each pair of adjacent chunks share an overlap of length $m/2$, and $m_i = m$ for all $i \in [k - 1]$, while $m/2 \leq m_k \leq m$. In this case, we have $k = \lceil 2n/m - 1 \rceil$.

Error metrics. Let us focus on how error metrics of the LLM-based algorithm are impacted by the hyperparameter m . We start by identifying two failure modes of each LLM call for retrieving the targeted information from a chunk of size m in Step 2 of the algorithm:

1. *The first failure mode* is that, while the needle is contained in the chunk, the LLM might mistakenly return “I don’t know” or an incorrect passcode. It is reasonable to expect that this failure mode will occur more frequently for larger values of m . Our early experiments with various LLMs confirmed that this failure mode starts to occur when m exceeds a certain threshold specific to each LLM.
2. *The second failure mode* is that, while the needle is actually absent from the chunk, the LLM might mistakenly return a passcode that it believes is the true answer to the question. We observed empirically that this is more likely to happen when the chunk contains some objects that seem similar to the targeted object (e.g. “red lock” or “green door” vs. “red door”), and that some LLMs are more prone to this failure mode even when the value of m is small, while others are less so.

Based on the above observations, we can hypothetically categorize LLMs into two types: *Type-1 LLMs* are only prone to the first failure mode, while *Type-2 LLMs* are prone to both. It turns out that analysis of error metrics for the overall LLM-based algorithm is dependent on the type of the LLM being used.

- Analysis is simpler if a Type-1 LLM is used: a smaller value of m means the first failure mode is less likely to occur in Step 2 of the algorithm, which implies higher accuracy for the final solution of the overall algorithm.
- Analysis is more complicated if a Type-2 LLM is used, since both failure modes can possibly occur in Step 2 of the algorithm. A larger value of m means the first failure mode is more likely to occur, while a smaller value of m implies a larger number of chunks $k = \lceil 2n/m - 1 \rceil$, which can potentially increase the chance of error in the final step of majority voting, due to the frequent occurrence of the second failure mode in Step 2 of the algorithm. Consequently, the minimum error of the overall algorithm might be achieved by some intermediate value of m that achieves a balance between the two failure modes. If n is too large, then there might not exist a good value of m that can achieve a low error, as either failure mode must occur with high probability.⁴

Cost metrics. Our analysis of cost metrics for this task is largely the same as that for the counting task, despite how different these two tasks might seem. Under some mild conditions explained in Section 3.1, most cost metrics of interest are monotonely decreasing in m , except for the end-to-end latency with parallel LLM calls, which is increasing in m for parallelism degree $p = \infty$ and possibly non-monotone for finite p . One thing to note is that, due to the overlaps between consecutive chunks, the number of parallel sub-tasks in Step 2 of the algorithm is $k = \lceil 2n/m - 1 \rceil$, rather than $\lceil n/m \rceil$ as in the counting task. This implies that the value of m minimizing the latency can be predicted by letting $2n/m - 1 \approx p$, namely $m \approx 2n/(p + 1)$.

3.5.3 Experiments

We validate our analysis with numerical experiments. For each task instance, the passcodes of all objects, the targeted object, the position of the haystack where the needle is inserted, etc., are all randomly chosen. The error metric of interest, namely the exact-match error, takes value 0 if the final solution of the algorithm is exactly the same as the ground-truth passcode to the targeted object, $1 - 1/h$ if the algorithm returns a list of h candidate solutions that includes the ground-truth passcode, and 1 otherwise.

Results with Llama-3-8B. Figure 8 includes the results of our experiments with Llama-3-8B.⁵

In Figure 8a, we vary the length n of the input text containing one needle in a haystack, and set $m = n$ for the LLM-based algorithm, which becomes equivalent to a single LLM call. Notice that the exact-match error, which corresponds to the first failure mode explained earlier, approaches zero as the problem size n decreases. In addition, the decoding length is $O(1)$, and the wall-clock latency is $O(\mathcal{L}_{\text{sys}} + n)$; one detailed observation is that as n increases, it becomes more likely that the LLM call returns “I don’t know”, which slightly decreases the number of decoding tokens and thus the latency.

Figure 8b includes the results for the same experiment setting, except that no needle is inserted into the haystack. One crucial observation is that the exact-match error in this case, which corresponds to the second

⁴An informal probabilistic analysis is as follows. Given the sub-task size m , denote the probability of the first and second failure modes as $p_1(m)$ and $p_2(m)$ respectively. Then, the success rate of retrieval for the chunk containing the needle is $1 - p_1(m)$, while the expected number of “false positives” from the remaining chunks is approximately $k \times p_2(m) \approx 2n \times p_2(m)/m$. One might opt for a relatively small value of m , which hopefully increases $1 - p_1(m)$ and hence mitigates the first failure mode. However, even if $p_2(m)/m$ is very small, say 10^{-3} , the number of false positives can still be large if the size n of the original problem is large, which will cause errors in the solution returned by majority voting.

⁵After executing many LLM calls in a row during our experiments with Llama-3-8B supported by ollama [oll23], we started to observe unusually large latencies (at least two orders of magnitude larger than their normal values) for some LLM calls, even though the generated texts are normal. We believe that this is most likely due to memory-related issues caused by running ollama on a laptop with limited 16GB memory, which can be easily avoided if a laptop with more memory is used. To mitigate this issue in our experiments, we take a different approach, i.e. adding a 3-second pause between each pair of consecutive LLM calls in the LLM-based algorithm when Llama-3-8B and ollama are used. While this proves to be quite effective, anomalies might still occur after running the experiments for a long period of time, in which case we simply re-run the part of experiments containing such anomalies, or remove these data points manually before plotting if there are very few of them,

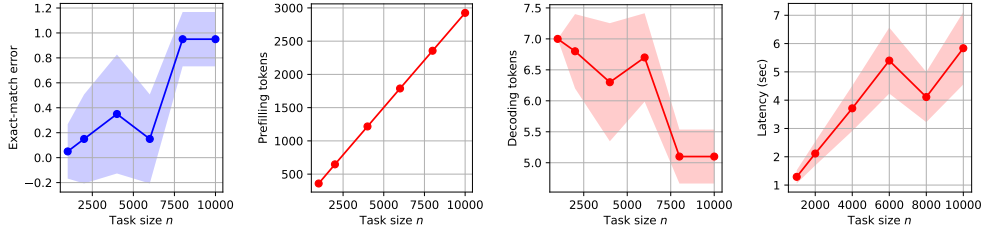
failure mode of retrieval, remains non-zero even for very small values of n . This suggests that Llama-3-8B should be regarded as a Type-2 LLM prone to both failure modes.

In Figures 8c and 8d, we vary the sub-task size m while n is fixed at 10000 and 20000 respectively. As was predicted by our analysis, the error of the overall algorithm is not monotone in the value of m , due to the presence of two failure modes. Another difference from the previous counting or sorting task is that the latency with parallelism degree $p = 4$ achieves the minimum around $m = 2n/(p + 1) = 0.4n$ rather than $m = n/p = 0.25n$, which again matches our previous analysis.

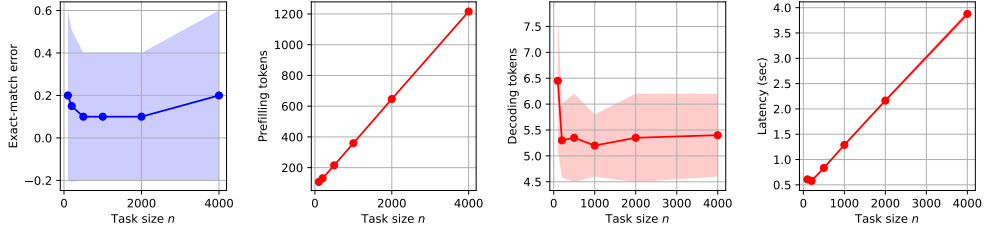
Results with Llama-3-70B. Figure 9 includes the results for the same experiments but with Llama-3-70B used within the LLM-based algorithm.

In particular, Figure 9a shows that Llama-3-70B achieves lower errors in the first failure mode of retrieval compared to Llama-3-8B, while Figure 9b suggests that Llama-3-70B is much less prone to the second failure mode and hence might be regarded as a Type-1 LLM. Consequently, in Figures 9c and 9d, the exact-match error exhibits a more monotone relation with the sub-task size m .

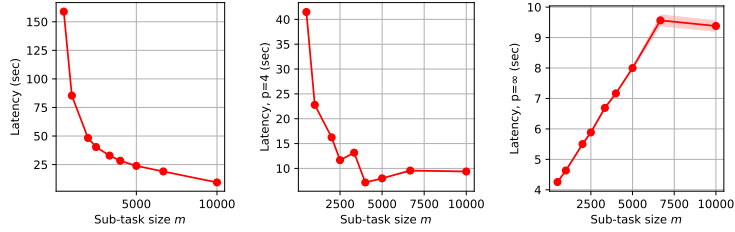
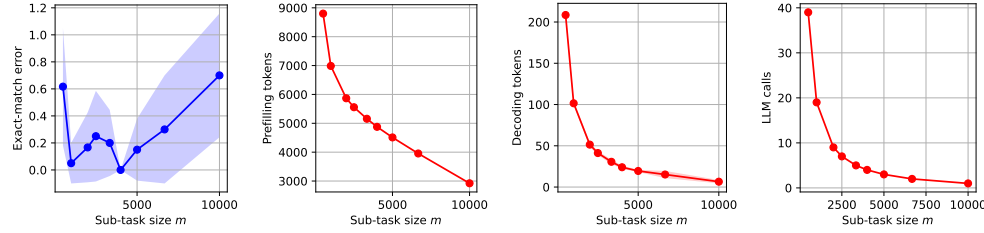
Regarding the cost metrics, results with Llama-3-70B are similar to those with Llama-3-8B.



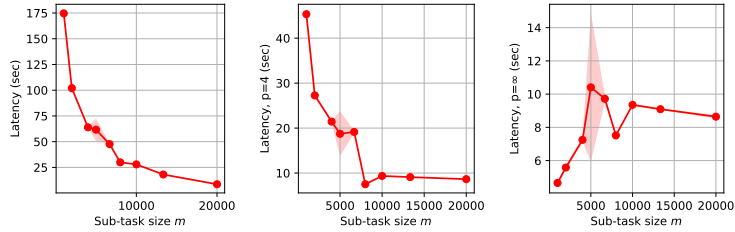
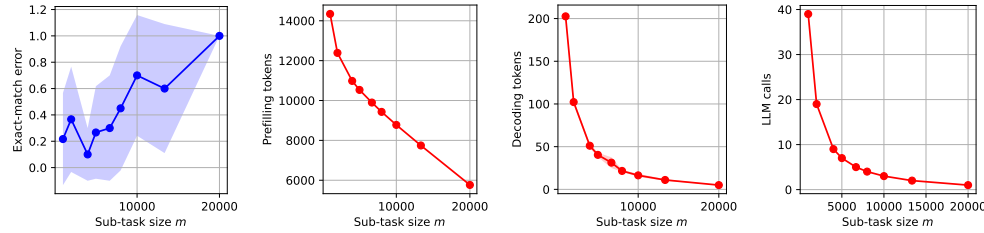
(a) Vary n and set $m = n$. (20 trials)



(b) Vary n and set $m = n$ for the no-needle case. (20 trials)

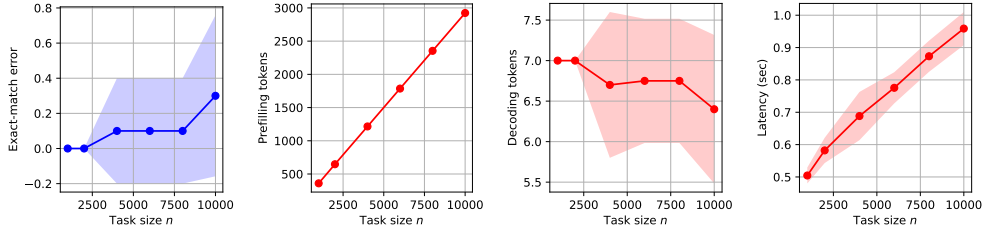


(c) Fix $n = 10000$ and vary m . (10 trials)

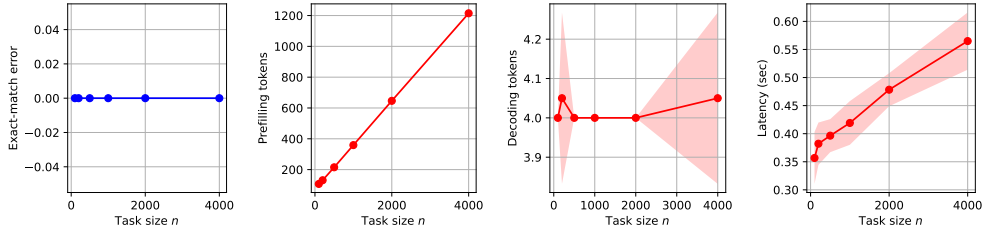


(d) Fix $n = 20000$ and vary m . (10 trials)

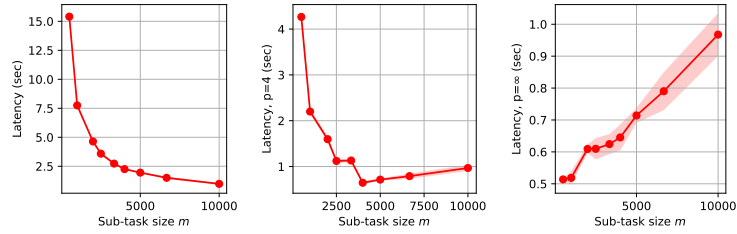
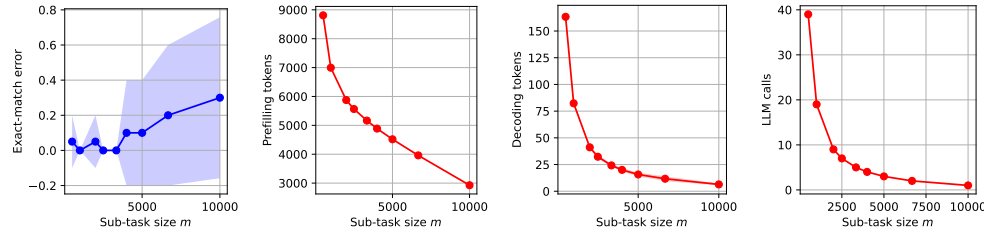
Figure 8: Empirical results for retrieval with Llama-3-8B.



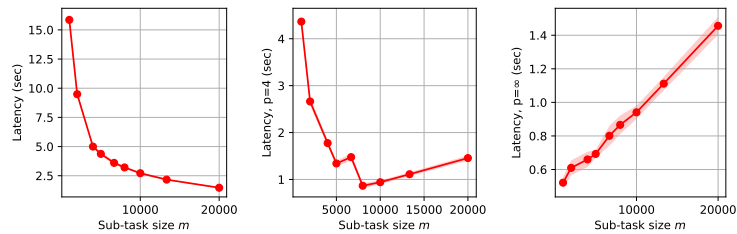
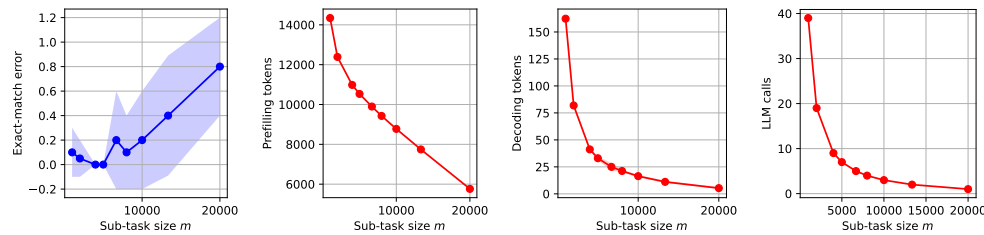
(a) Vary n and set $m = n$. (20 trials)



(b) Vary n and set $m = n$ for the no-needle case. (20 trials)



(c) Fix $n = 10000$ and vary m . (10 trials)



(d) Fix $n = 20000$ and vary m . (10 trials)

Figure 9: Empirical results for retrieval with Llama-3-70B.

3.6 Example: retrieval-augmented generation

Our next example is a multiple-needle generalization of the previous retrieval task, which can be regarded as a synthetic and simplified version of retrieval-augmented generation (RAG) [LPP+20, GXG+24]. In particular, we consider fine-grained sentence-level retrieval by LLMs, rather than document-level or chunk-level retrieval by certain similarity measure of dense embedding vectors.

More concretely, suppose that the input text is composed of sentences of the form “The $\{i\}$ -th digit of the passcode to the $\{\text{colored object}\}$ is $\{\text{digit}\}$ ”, where $i \in [6]$. The algorithm is asked to answer the question “What is the 6-digit passcode to the $\{\text{targeted object}\}$?”. Compared with the previous single-needle retrieval task, here the algorithm need to retrieve multiple needles, each for one digit of the targeted object, in order to answer the question correctly; moreover, the final aggregation step requires certain capability of reasoning or summarization over the retrieved needles.

Note again that while we focus on this specific setting in our experiments, the algorithm and analysis in the following are actually applicable to generic settings of this RAG task.

3.6.1 Algorithm

We consider the following LLM-based algorithm for solving this task:

1. Divide the input text of length n into k overlapping chunks of lengths m_1, \dots, m_k ;
2. For each chunk, use one LLM call to retrieve sentences that can be useful for answering the question;
3. Put the retrieved sentences together, based on which one LLM call is invoked for answering the question.

We note a few details about this algorithm. (1) For each chunk in Step 2, we prompt the LLM to retrieve relevant sentences, or return “None” if no relevant sentence is found in that chunk. Such “None” results will be excluded from Step 3 of the algorithm. (2) Unlike previous examples, the final aggregation step of this algorithm involves an LLM node, which adds to the cost metrics of the overall algorithm. (3) For simplicity, we assume that the number of needles (i.e. length of the passcode) and the length of each needle are both $O(1)$. For more general cases, the final aggregation step might benefit from further task decomposition. (4) We allow the algorithm to return a partial answer, by placing a special character in the digit(s) of the passcode that it is uncertain about.

3.6.2 Analysis

Let us assume for concreteness that each pair of adjacent chunks share an overlap of length $m/2$, and $m_i = m$ for all $i \in [k - 1]$, while $m/2 \leq m_k \leq m$. In this case, we have $k = \lceil 2n/m - 1 \rceil$.

Error metrics. Our analysis of error metrics for this task is similar to that for the previous retrieval example. In particular, there are two possible failure modes in the retrieval step, and conclusions for the errors of the final solution returned by the overall algorithm are dependent on whether a Type-1 or Type-2 LLM is being used. For example, if a Type-1 LLM, which will not mistakenly retrieve irrelevant sentences from the input text, is used within the algorithm, then a smaller value of m implies higher accuracy of retrieval in Step 2 of the algorithm, which further leads to lower error metrics for the solution returned by the final aggregation step.

Cost metrics. For simplicity, let us assume that a Type-1 LLM is used within the overall algorithm. Consequently, in Step 2 of the algorithm, each LLM call has $\mathcal{L}_{\text{pre}} \leq \mathcal{L}_{\text{sys}} + O(m)$ and $\mathcal{L}_{\text{dec}} = O(1)$, since only the relevant text within the chunk is retrieved. Moreover, among the k LLM calls, only $O(1)$ of them return answers that are not “None”. By excluding the “None” results from the final aggregation step, the last LLM call has $\mathcal{L}_{\text{pre}} \leq \mathcal{L}_{\text{sys}} + O(1)$ and $\mathcal{L}_{\text{dec}} = O(1)$. Putting things together, with a degree of parallelism p and the number of chunks $k = \lceil 2n/m - 1 \rceil$, the cost metric \mathcal{C} of the overall algorithm is bounded by

$$\begin{aligned} \mathcal{C} &= \mathcal{C}(\text{sub-tasks}) + \mathcal{C}(\text{aggregation}), \quad \text{where} \\ \mathcal{C}(\text{sub-tasks}) &\leq \left\lceil \frac{k}{p} \right\rceil \times \left(\mathcal{C}_{\text{pre}}(\mathcal{L}_{\text{sys}} + m) + \mathcal{C}_{\text{dec}}(\mathcal{L}_{\text{sys}} + m, 1) \right), \end{aligned}$$

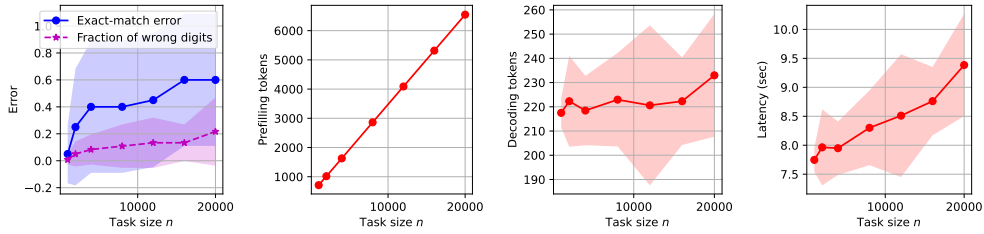
$$\mathcal{C}(\text{aggregation}) \leq \mathcal{C}_{\text{pre}}(\mathcal{L}_{\text{sys}} + 1) + \mathcal{C}_{\text{dec}}(\mathcal{L}_{\text{sys}} + 1, 1).$$

3.6.3 Experiments

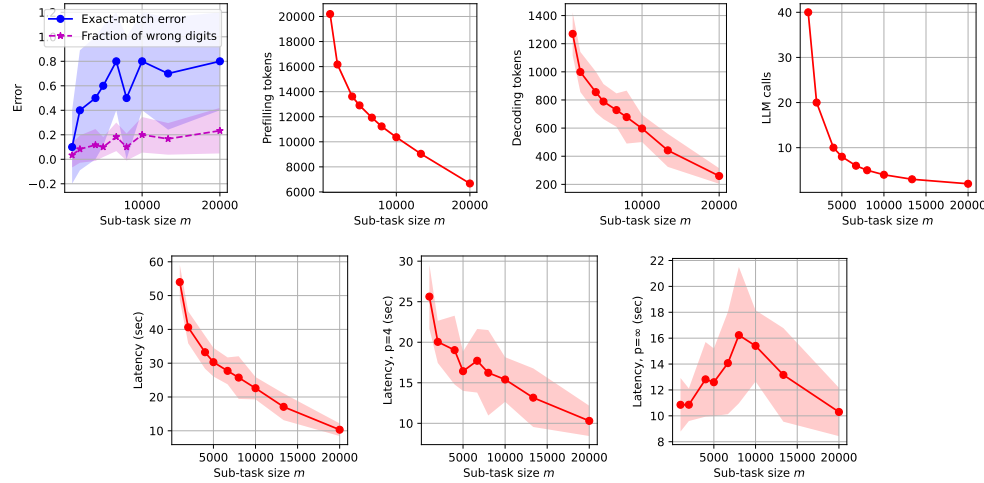
We empirically validate the performance of the proposed LLM-based algorithm with a Llama-3-70B model. Two error metrics are considered: the exact-match error taking value in $\{0, 1\}$, and the fraction of incorrect digits, which takes value in $[0, 1]$ and is always no larger than the exact-match error.

In Figure 10a, we vary the problem size n , and set $m = n$ in the LLM-based algorithm. It is observed that the error metrics are monotonely increasing in n , and approach zero as n decreases. Most cost metrics are also increasing in n , except for the number of decoding tokens, which is supposed to be determined by the number and lengths of the needles only, not the haystack, and thus should be insensitive to n .

In Figure 10b, we fix $n = 20000$ and vary the chunk size m . As was predicted by our analysis for a Type-1 LLM, a smaller value of m implies lower error metrics, indicating the efficacy of task decomposition.



(a) Vary n and set $m = n$. (20 trials)



(b) Fix $n = 20000$ and vary m . (10 trials)

Figure 10: Empirical results for RAG with Llama-3-70B.

3.7 Example: long-text summarization with chunking

For the final example of this section, we apply our analytical framework to the task of long-text summarization [KRA+22, CLGI24], where generating a summary for the long input text with a single LLM call is infeasible. Algorithms that process the long text to be summarized by chunks have been proposed, such as hierarchical merging [WOZ+21] and incremental updating [Ope24b]. The former first generates one summary for each chunk independently and then merge these intermediate summaries into the final one, while the latter maintains and updates a global summary as the chunks get processed one by one in order. Since objective and quantitative evaluation for the summarization task is known to be challenging [CLGI24] and remains an active research area, we focus our study on the cost metrics of both algorithms. Our analysis leads to interesting observations that are different from those in previous examples, primarily due to the various options of setting the number of generated tokens \mathcal{L}_{dec} for each LLM call within the algorithms.

3.7.1 Processing chunks in parallel

Algorithm. Let us consider the following algorithm that processes the chunks in parallel, which is a simplification of hierarchical merging [CLGI24] and visualized in Figure 2a:

1. Divide the input text of length n into k chunks of length m_1, m_2, \dots, m_k .
2. Summarize each chunk with one LLM call, independently and in parallel. For the i -th chunk, the LLM is prompted to generate a summary of length no larger than s_i .
3. Invoke one LLM call to merge the summaries into a single summary of length no larger than s .

Note that the targeted lengths of the intermediate and final summaries, denoted by $\{s_i\}_{i \in [k]}$ and s , are hyperparameters of the algorithm that need to be pre-specified, in addition to the number of chunks k and the chunk sizes $\{m_i\}_{i \in [k]}$.

Analysis. For notational convenience, we assume that the chunk sizes satisfy $m_i \asymp m := n/k$ for all $i \in [k]$.

First, consider each individual LLM call: the cost of summarizing the i -th chunk can be bounded by $\mathcal{C}_{\text{LLM}}(\mathcal{L}_{\text{sys}} + m, s_i)$, while the cost of the final merging step can be bounded by $\mathcal{C}_{\text{LLM}}(\mathcal{L}_{\text{sys}} + \sum_{i \in [k]} s_i, s)$. To further simplify notations, we assume that $s_i = s_1$ for all $i \in [k]$, which will soon be justified. Then the total cost \mathcal{C} of the overall algorithm can be bounded by

$$\begin{aligned} \mathcal{C} &\leq \mathcal{C}(\text{summarize chunks}) + \mathcal{C}(\text{merge summaries}) \\ &= k \times \mathcal{C}_{\text{LLM}}(\mathcal{L}_{\text{sys}} + m, s_1) + \mathcal{C}_{\text{LLM}}(\mathcal{L}_{\text{sys}} + k \times s_1, s), \end{aligned}$$

while the end-to-end latency with parallelism degree p can be bounded by

$$\mathcal{C} \leq \lceil \frac{k}{p} \rceil \times \mathcal{C}_{\text{LLM}}(\mathcal{L}_{\text{sys}} + m, s_1) + \mathcal{C}_{\text{LLM}}(\mathcal{L}_{\text{sys}} + k \times s_1, s).$$

Let us specify the hyperparameters s_1 and more generally $\{s_i\}$, assuming that the targeted length s of the final summary has been determined. If the targeted information that we wish to be included in the final summary is distributed evenly across the input text, e.g. in a story with a linear narrative, then it is reasonable to set $s_i = s_1 = s/k$ for all $i \in [k]$. In other scenarios where the targeted information is distributed unevenly (e.g. in query-focused summarization [LFXW24, VFK+22]), it is generally safer to set $s_i = s_1 = s$ for all $i \in [k]$. The latency with parallelism degree p in both cases is summarized as follows:

$$\mathcal{C} \leq \begin{cases} \lceil k/p \rceil \times \mathcal{C}_{\text{LLM}}(\mathcal{L}_{\text{sys}} + m, s/k) + \mathcal{C}_{\text{LLM}}(\mathcal{L}_{\text{sys}} + s, s) & \text{if } s_1 = s/k, \\ \lceil k/p \rceil \times \mathcal{C}_{\text{LLM}}(\mathcal{L}_{\text{sys}} + m, s) + \mathcal{C}_{\text{LLM}}(\mathcal{L}_{\text{sys}} + k \times s, s) & \text{if } s_1 = s. \end{cases}$$

Further analysis can be derived from here. To give an example, let us focus on the case of $s_1 = s$ and try to find the chunk size m that minimizes the latency with parallelism degree p . For simplicity, we ignore

the length \mathcal{L}_{sys} of the system prompt and the limit \bar{m} on the context window size. We also assume that the time complexity of each LLM call is linear, namely $\mathcal{C}_{\text{LLM}}(\mathcal{L}_{\text{pre}}, \mathcal{L}_{\text{dec}}) \lesssim \mathcal{L}_{\text{pre}} + \mathcal{L}_{\text{dec}}$. Then we have

$$\mathcal{C} \leq \lceil \frac{k}{p} \rceil \times \mathcal{C}_{\text{LLM}}(\mathcal{L}_{\text{sys}} + m, s) + \mathcal{C}_{\text{LLM}}(\mathcal{L}_{\text{sys}} + k \times s, s) \lesssim \lceil \frac{k}{p} \rceil \times (m + s) + k \times s.$$

Even in such an oversimplified case, finding the optimal chunk size m is non-trivial:

- For large $m \geq \tilde{m} := n/p$ such that $k = n/m < p$, we have $\lceil k/p \rceil = 1$, and hence

$$\mathcal{C} \lesssim m + s + k \times s = m + \frac{n \times s}{m} + s.$$

The right-hand side attains the minimum at $\hat{m} := \sqrt{n \times s}$.

- For small $m < \tilde{m} = n/p$, we have the approximation $\lceil k/p \rceil \approx k/p$, and hence

$$\begin{aligned} \mathcal{C} &\lesssim \frac{k}{p} \times (m + s) + k \times s = k \times \left(\frac{m}{p} + \left(\frac{1}{p} + 1 \right) \times s \right) \\ &\lesssim \frac{n}{m} \times \left(\frac{m}{p} + s \right) = n \times \left(\frac{1}{p} + \frac{s}{m} \right). \end{aligned}$$

The right-hand side is monotonely decreasing in m .

Given the above, it can be verified that the optimal chunk size m^* that minimizes the latency \mathcal{C} can be estimated by $m^* \asymp \max\{\hat{m}, \tilde{m}\} = \max\{\sqrt{n \times s}, n/p\}$.

3.7.2 Processing chunks sequentially

Algorithm. Let us consider the following algorithm that processes the chunks sequentially, which is a simplification of incremental updating [CLGI24] and visualized in Figure 2b:

1. Divide the input text of length n into k chunks of length m_1, m_2, \dots, m_k .
2. Initialize the global summary as an empty string, and update it incrementally via processing the chunks in order: at the i -th iteration, invoke one LLM call to utilize the global summary and the i -th chunk for generating a new global summary of length no larger than s_i .
3. The output of the overall algorithm is that of the final LLM call for summarizing the last chunk.

Analysis. While this algorithm clearly has a sequential nature, our previous analysis for parallel decomposition can be easily adapted for this case. For the i -th step of updating the global summary, we have $\mathcal{L}_{\text{pre}} \leq \mathcal{L}_{\text{sys}} + m + s_{i-1}$ and $\mathcal{L}_{\text{dec}} \leq s_i$, and thus its cost is bounded by

$$\mathcal{C}_i \leq \mathcal{C}_{\text{LLM}}(\mathcal{L}_{\text{sys}} + m + s_{i-1}, s_i).$$

Therefore, the total cost of the overall algorithm satisfies

$$\mathcal{C} \leq \sum_{i \in [k]} \mathcal{C}_i \leq \sum_{i \in [k]} \mathcal{C}_{\text{LLM}}(\mathcal{L}_{\text{sys}} + m + s_{i-1}, s_i).$$

Further analysis can provide insights for choosing the hyperparameters that minimize the total cost, though we omit the details here to avoid repetition.

4 Case study: hierarchical decomposition

This section studies the pattern of *hierarchical decomposition* for LLM-based algorithms, where the original task is decomposed into multiple sub-tasks, and each of them can be further decomposed into more lower-level sub-tasks. This pattern is strictly more expressive than parallel decomposition studied in the previous section, and hence capable of solving more problems.

For concreteness, we investigate a challenging version of the RAG task studied in Section 3.6 that requires multi-hop reasoning [YQZ⁺18, LZLC24]. Recall that in the previous RAG example, given a question and multiple text chunks, the algorithm following the pattern of parallel decomposition will first retrieve useful sentences from each chunk, and then invoke one LLM call to answer the question based on the retrieved information. Such a method might not be feasible in more challenging scenarios, where the needles embedded in the haystack are logically related, and some of the needles are related to the targeted question only *indirectly* via connection to other needles. For example, suppose that the question is “what is the numeric value of A”, while the needles are “A = B”, “B = C”, and “C = 100”, located separately in different chunks. Retrieving needles from their corresponding chunks solely based on the targeted question will certainly fail in this case.

To tackle this challenge, a natural idea is to extend the RAG algorithm considered in Section 3.6, allowing it to perform multiple rounds of iterative retrieval and reasoning. For each round, the algorithm performs retrieval based on the targeted question as well as additional information from previous rounds, followed by reasoning about the retrieved sentences and deciding whether the targeted question can be answered, or further retrieval and reasoning is needed. Similar approaches have been widely adopted in prior work, e.g. in the Selection-Inference framework [CSH23], in a RAG system with iterative follow-up questions for applications in medicine [XJW⁺24], or as a technique of extending the effective context window of a LLM-powered agent system [QT24]. The resulting algorithm for reasoning with iterative retrieval exhibits a hierarchical structure: the original task is decomposed into multiple sequential rounds, and each round is further decomposed into multiple steps of retrieval and reasoning.

In the rest of this section, we first elaborate the concrete setup and algorithms for this case study, and then demonstrate our analysis of accuracy and efficiency based on the proposed analytical framework, as well as insights derived from it. Finally, numerical experiments are conducted to validate the efficacy and scalability of the considered algorithm, as well as our analysis and insights.

4.1 Concrete setup

For concreteness, let us consider the task of finding the numeric value of a targeted variable embedded within a grid, similar to the setting considered in [YXLAZ24]. A visualization can be found in Figure 11. Configurations of the grid include its depth d , width w , and degree g , which control the difficulty of this task. More specifically, the grid consists of d levels, each containing w variables; each variable at a certain level is a function (e.g. addition, subtraction, maximum or minimum) of g variables at the next level, except for the variables at the final level, whose numeric values are given. Such information is provided in clues of the form “A2 = B1 + B3” or “C1 = 10”, each of which corresponds to one variable. As a result, the total number of clues is $d \times w$, and each clue has length $O(g)$. We refer to the clues that are necessary and sufficient for calculating the targeted variable as the needles, which constitute a directed acyclic graph (DAG) embedded within the grid. It is assumed that the level of reasoning required in this case study is non-trivial yet also simple enough, in the sense that one single LLM call with step-by-step reasoning is sufficient for answering the targeted question correctly if all needles are given *a priori*.

4.2 Algorithm

To solve this task, we consider an LLM-based algorithm that involves multiple rounds of retrieval and reasoning, which is visualized in Figure 12 and explained in the following:

1. Divide the input clues into k chunks. In addition, initialize an empty list of references, i.e. clues retrieved by LLM calls, which will be maintained and updated throughout the algorithm.

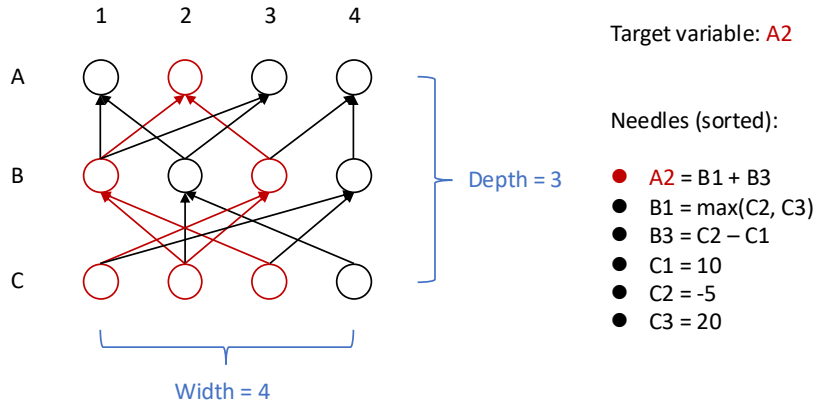


Figure 11: An example grid of variables with depth $d = 3$, width $w = 4$, and degree $g = 2$. The targeted variable is A_2 at the top level, which is a function of B_1 and B_3 at the next level. The variables whose numeric values are necessary and sufficient for calculating A_2 are highlighted in red, and their corresponding clues constitute a DAG of needles.

2. For each round of the algorithm, invoke k sequential (Figure 12a) or parallel (Figure 12b) LLM calls for retrieval from k chunks based on the targeted question and references, then invoke one LLM call to reason about the updated references and try to answer the targeted question.
 - If the LLM returns an answer, then the overall algorithm outputs that answer and terminate.
 - If the LLM cannot answer, and no additional clue has been retrieved in this round, then the algorithm terminates and fails⁶.
 - Otherwise, move on to the next round of retrieval and reasoning, with the updated references.

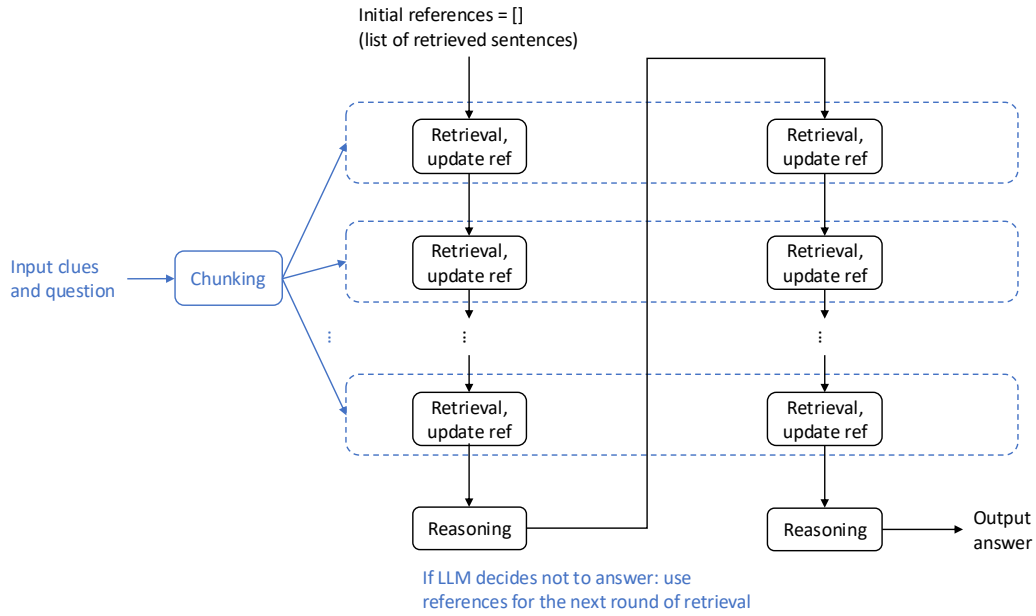
Options for reasoning and answering. We consider two options of prompting the LLM to reason about the references and answer the targeted question: answering directly, or thinking step by step before answering [KGR⁺22]. It is reasonable to expect that the latter will boost the accuracy while incurring higher costs, which will soon be investigated analytically and quantitatively in Section 4.3.

Options for retrieval. We consider two options, referred to as “cyclic” and “parallel”, for retrieval from multiple chunks during each round of the algorithm.

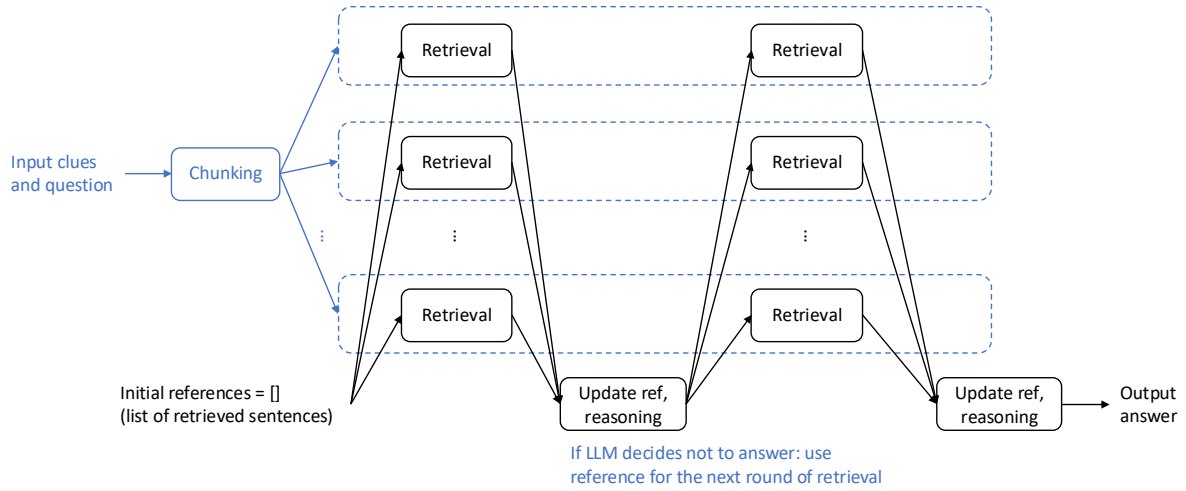
- With the “cyclic” option (Figure 12a), chunks are processed sequentially; more specifically, after retrieval for each chunk, the retrieved clues are added to the list of references immediately, before retrieval for the next chunk starts. Consequently, the chunks are processed in a cyclic manner throughout the overall algorithm, which gives rise to the name of this option.
- With the “parallel” option (Figure 12b), chunks are processed independently and in parallel, after which the list of references is updated once. This exemplifies using parallel decomposition (cf. Section 3) as a building block for more complicated LLM-based algorithms.

With the “cyclic” option, the overall algorithm typically need fewer rounds to answer the targeted question correctly, since each LLM call for retrieval always leverages the most updated references. On the other hand, the “parallel” option can leverage parallelism of LLM calls for reducing the end-to-end latency of the overall algorithm. The comparison between these two options will soon be elaborated in Section 4.3.

⁶This is due to the assumption that greedy decoding, which is deterministic, is adopted. In this case, running one more round of retrieval and reasoning will give the same result as that of the current round, which will be useless and wasteful. A potential improvement is to adaptively decrease (e.g. halve) the chunk size and continue the algorithm with more rounds; such improvements are not the focus of this work, and hence omitted here.



(a) The “cyclic” version.



(b) The “parallel” version.

Figure 12: Algorithms for reasoning with iterative retrieval, which exhibit the pattern of hierarchical decomposition. While the number of rounds is assumed to be 2 in this visualization, it is actually determined adaptively by the algorithm itself at runtime. For clarity of visualization, some LLM or non-LLM nodes (cf. Figure 1) are merged into one, and an arrow from the “chunking” node to a dashed block means that each “retrieval” node within the dashed block takes the corresponding chunk as input.

Remark 3. The algorithm under consideration exhibits the pattern of hierarchical decomposition, in that the overall task is decomposed into a sequence of rounds, and each round is further decomposed into multiple steps of retrieval and reasoning. Another feature of this algorithm is that its computational graph is constructed dynamically at runtime, since the number of rounds is determined adaptively by the algorithm itself.

4.3 Analysis

4.3.1 Error metrics

There are two major failure modes for this algorithm of reasoning with iterative retrieval:

- *Mistakes in reasoning and answering.* For example, the LLM call responsible for reasoning and answering might mistakenly decide that it is not yet ready to answer the targeted question, or make mistakes when doing the arithmetic and thus return a wrong numeric value, even when all needles have been successfully retrieved. It is also possible that the LLM call mistakenly returns a numeric value (e.g. the value of a variable whose name is similar to that of the targeted variable), while the needles have not been fully retrieved yet. The probability of this failure mode is particularly related to whether the LLM call responsible for reasoning and answering is prompted to answer directly or think step by step before answering.
- *Failure to retrieve all needles.* As long as the ground-truth DAG of needles has a limited size, the probability of this failure mode is largely determined by the choice of the chunk size. Since this has been thoroughly investigated in our previous retrieval (Section 3.5) and RAG (Section 3.6) examples, it will not be our focus in this section.

4.3.2 Cost metrics

Notations. Recall from Eq. (2) that $\mathcal{C}_{\text{LLM}}(\mathcal{L}_{\text{pre}}, \mathcal{L}_{\text{dec}}) = \mathcal{C}_{\text{pre}}(\mathcal{L}_{\text{pre}}) + \mathcal{C}_{\text{dec}}(\mathcal{L}_{\text{pre}}, \mathcal{L}_{\text{dec}})$ stands for the cost of one LLM call with a prompt of length \mathcal{L}_{pre} and generated text of length \mathcal{L}_{dec} . We also adopt some notations from Section 3.1 in our previous study of parallel decomposition: n represents the total length (in tokens or characters) of the input clues, m represents an upper bound for the chunk size, $k \lesssim n/m$ denotes the number of chunks, and \mathcal{L}_{sys} denotes an upper bound for the length of the system prompt for each LLM call.

In addition, let r denote the number of rounds, which is determined adaptively by the algorithm itself at runtime. Finally, let ℓ be the total length of the needles, i.e. clues that are necessary and sufficient for answering the targeted question correctly. The value of ℓ can depend on the depth d , width w and degree g of the grid in various ways:

- If $g = 1$, then the needles form a chain of length d , in the form of “A = B”, “B = C”, “C = D”, and so on. In this case, we have $\ell \lesssim d$.
- If the width $w > d^{g-1}$ is sufficiently large, then the number of needles can be upper bounded by the size of a tree with d levels and g children per node, namely $1 + g + g^2 + \dots + g^{d-1} = (g^d - 1)/(g - 1)$. Since each needle has length $O(g)$, we have $\ell \lesssim g \times (g^d - 1)/(g - 1)$.
- If the width $w \ll d^{g-1}$ is limited, then a tighter bound for the number of needles will be $d \times w$, and thus $\ell \lesssim g \times d \times w$.

The “cyclic” version (Figure 12a). Let us first study the cost of each LLM call.

- An LLM call responsible for retrieval takes one chunk and the references as input, which has length $O(m + \ell)$. In addition, it is supposed to output a list of clues, which has length $O(\ell)$, that is relevant to the targeted question. In other words, we have $\mathcal{L}_{\text{pre}} \leq \mathcal{L}_{\text{sys}} + O(m + \ell)$, $\mathcal{L}_{\text{dec}} \lesssim \ell$, and thus

$$\mathcal{C}(\text{retrieval}) \leq \mathcal{C}_{\text{LLM}}(\mathcal{L}_{\text{sys}} + m + \ell, \ell)$$

- An LLM call responsible for reasoning and answering takes the references of length $O(\ell)$ as input, namely $\mathcal{L}_{\text{pre}} \leq \mathcal{L}_{\text{sys}} + O(\ell)$. As for the length of generated text \mathcal{L}_{dec} , it is reasonable to assume that

$\mathcal{L}_{\text{dec}} \lesssim 1$ if the LLM is prompted to answer directly, and $\mathcal{L}_{\text{dec}} \lesssim \ell$ if it is prompted to do the calculation step by step before returning its final answer⁷. Consequently, one has

$$\mathcal{C}(\text{reasoning}) \leq \mathcal{C}_{\text{LLM}}(\mathcal{L}_{\text{sys}} + \ell, 1 \text{ or } \ell).$$

Now we are ready to find out the cost of the overall algorithm with r rounds of iterative retrieval (for k chunks) and reasoning:

$$\begin{aligned} \mathcal{C} &\leq r \times \mathcal{C}(\text{one round}) \\ &= r \times \left(k \times \mathcal{C}(\text{retrieval}) + \mathcal{C}(\text{reasoning}) \right) \\ &\leq r \times \left(k \times \mathcal{C}_{\text{LLM}}(\mathcal{L}_{\text{sys}} + m + \ell, \ell) + \mathcal{C}_{\text{LLM}}(\mathcal{L}_{\text{sys}} + \ell, 1 \text{ or } \ell) \right). \end{aligned}$$

In particular, this bound quantifies how the cost of LLM calls responsible for reasoning and answering, namely $r \times \mathcal{C}_{\text{LLM}}(\mathcal{L}_{\text{sys}} + \ell, 1 \text{ or } \ell)$, only occupies a small fraction of the total cost of the overall algorithm.

The “parallel” version (Figure 12b). Analysis of cost metrics for the “parallel” version is largely the same as that for the “cyclic” version, with the following two major differences:

- For the same task instance, the “parallel” version requires the same or a larger number of rounds, since in the “cyclic” version, each retrieval step always leverages the most updated references. For example, consider the case with degree $g = 1$ and a chain of d needles located separately in different chunks. Then, the number of rounds will be $r = d$ for the “parallel” version, but can be as small as $r = 1$ for the “cyclic” version, if the needles happen to appear in the right order in the original clues.
- If the cost metric of interest is the end-to-end latency with parallelism degree p , then the k LLM calls for retrieval within each round can be parallelized, which implies

$$\begin{aligned} \mathcal{C} &\leq r \times \left(\left\lceil \frac{k}{p} \right\rceil \times \mathcal{C}(\text{retrieval}) + \mathcal{C}(\text{reasoning}) \right) \\ &\leq r \times \left(\left\lceil \frac{k}{p} \right\rceil \times \mathcal{C}_{\text{LLM}}(\mathcal{L}_{\text{sys}} + m + \ell, \ell) + \mathcal{C}_{\text{LLM}}(\mathcal{L}_{\text{sys}} + \ell, 1 \text{ or } \ell) \right). \end{aligned} \quad (6)$$

As a result, the end-to-end latency of the “parallel” version with a sufficiently large parallelism degree p can be potentially smaller than that of the “cyclic” version.

4.3.3 Insights

In sum, we derive two major insights from the above analysis of error and cost metrics:

1. LLM nodes responsible for reasoning and answering only occupy a small fraction of the costs of the overall algorithm, while playing a critical role in the output of the algorithm and thus in the error metrics. Therefore, our general recommendation is to prompt these LLM calls to think step by step before answering, instead of answering directly, which will most likely boost the accuracy significantly with negligible loss in efficiency.
2. Regarding the “cyclic” and “parallel” options for retrieval, we conclude that each of them has its own pros and cons. With the “cyclic” option, fewer rounds of retrieval and reasoning are needed (thanks to the timely updates to the references), but the downside is that all retrieval steps have to be executed sequentially. In contrast, with the “parallel” option, the algorithm typically requires more rounds of retrieval and reasoning and thus larger costs in terms of most metrics, but can leverage parallelism of LLM calls for reducing the end-to-end latency. Therefore, whether the “cyclic” or “parallel” option is preferred largely depends on which cost metric is of more concern.

⁷There might exist more precise characterizations of \mathcal{L}_{dec} in this case, e.g. $\mathcal{L}_{\text{dec}} \lesssim \ell \times g$ if the LLM tends to take g steps for calculating the sum of g numbers. For simplicity, we mostly assume $g = O(1)$ in this case study, and thus stick to the assumption that $\mathcal{L}_{\text{dec}} \lesssim \ell$.

4.4 Experiments

We validate our analysis via experiments with a `Qwen-2-72B-Instruct` model [YYH+24], supported by vLLM [KLZ+23] and running on a server with 4 Nvidia A100-80G GPUs. For each experiment, we vary the depth, width or degree of the grid of variables (which controls the difficulty of task instances), while validating Insight 1 by comparing two options for prompting LLM calls that are responsible for reasoning and answering, or Insight 2 by comparing the “cyclic” and “parallel” options for retrieval.

Error metrics of interest include (1) the exact-match error, which takes value 0 if the answer returned by the algorithm matches the ground-truth solution exactly, and value 1 otherwise; (2) the absolute error, i.e. the absolute value of the difference between the algorithm’s answer and the ground-truth solution; and (3) the missed-coverage error, i.e. the ratio of needles that the algorithm fails to retrieve and hence are not included in the references maintained by the algorithm. Note that missed coverage might arise not just from failures of the LLM calls responsible for retrieval, but also from the possibility that the algorithm terminates too early with fewer rounds than necessary, due to hallucination by the LLM calls responsible for reasoning and answering. Cost metrics of interest are the same as those explained in Section 3.2, plus the number of rounds, a metric specific to the hierarchical pattern of algorithms considered in this section.

Remark 4 (Mitigating hallucination in retrieval). During our early experiments, we observed that LLMs tend to make up clues not present in the input during the retrieval steps. To address this, we prompt the LLM to return exact copies of clues from the original text, and further use a symbolic program to check whether the retrieved clues are indeed exact copies (which, from the perspective of LLM-powered agent systems, might be regarded as tool use). Only those passing the test will be added to the list of references. It has been confirmed empirically that this simple method effectively mitigates the errors caused by hallucination of LLMs during retrieval, making the overall algorithm much more robust and accurate in our experiments.

Comparing two prompting options. For this experiment, we consider shallow and wide grids of variables, with depth $d = 2$ and width $w = 300$. The degree g varies, controlling the difficulty in arithmetic. The algorithm uses a fixed chunk size of 50 clues, and the “parallel” version of retrieval. In this case, the number of rounds should be 2 if each retrieval step succeeds.

Empirical results for this experiment are illustrated in Figure 13, which confirm Insight 1, i.e. prompting the LLM to think step by step for reasoning and answering significantly boosts the accuracy of the overall algorithm while incurring minor overhead in cost metrics, compared to answering directly. Note from the last row, though, that the relative difference in terms of end-to-end latencies increases with the parallelism degree p , which has been predicted by our analysis, in particular Eq. (6).

Comparing the “cyclic” and “parallel” versions. In the following experiments, we consider grids with fixed degree $g = 1$ and thus chains of needles. We either fix the depth $d = 5$ and vary the width w , or fix the width $w = 100$ and vary the depth d . The algorithm uses a fixed chunk size of 100 clues, and prompts the LLM calls responsible for reasoning and answering to think step by step.

Empirical results for these two experiments can be found in Figures 14 and 15, which confirm that the considered algorithm achieves high accuracy for a wide range of task configurations. Insight 2 from our analysis is also validated: compared with the “cyclic” version, the “parallel” version incurs a larger number of rounds and hence higher cost metrics, except for the end-to-end latencies with parallelism, for which the benefits of parallelism outweigh the downside of requiring more rounds.

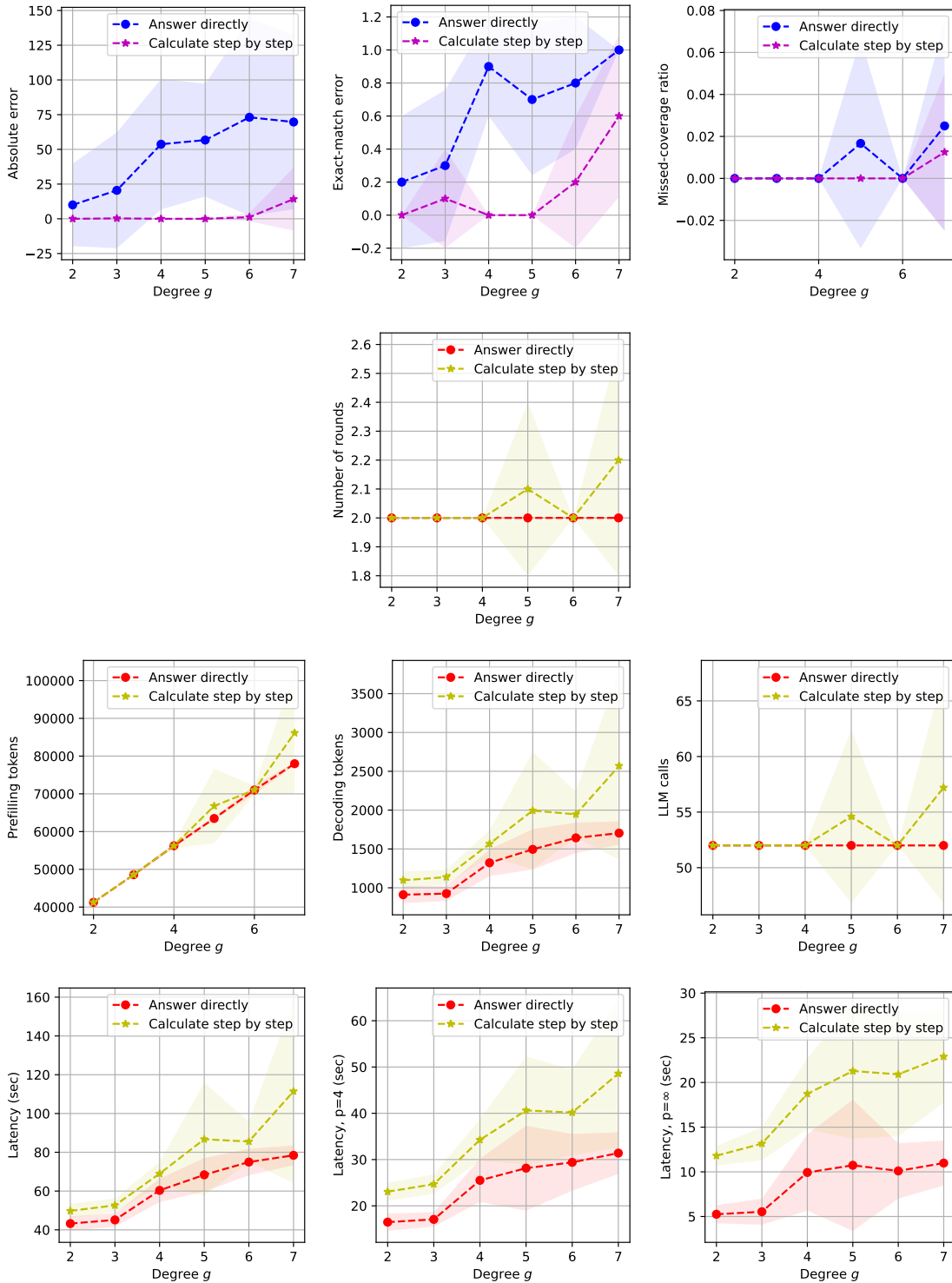


Figure 13: Empirical results (10 trials) for reasoning with iterative retrieval, where two options of prompting the LLM calls responsible for reasoning and answering are compared. The depth $d = 2$ and width $w = 300$ are fixed, while the degree g varies. The algorithm uses a chunk size of 50 clues, and the “parallel” version of retrieval.

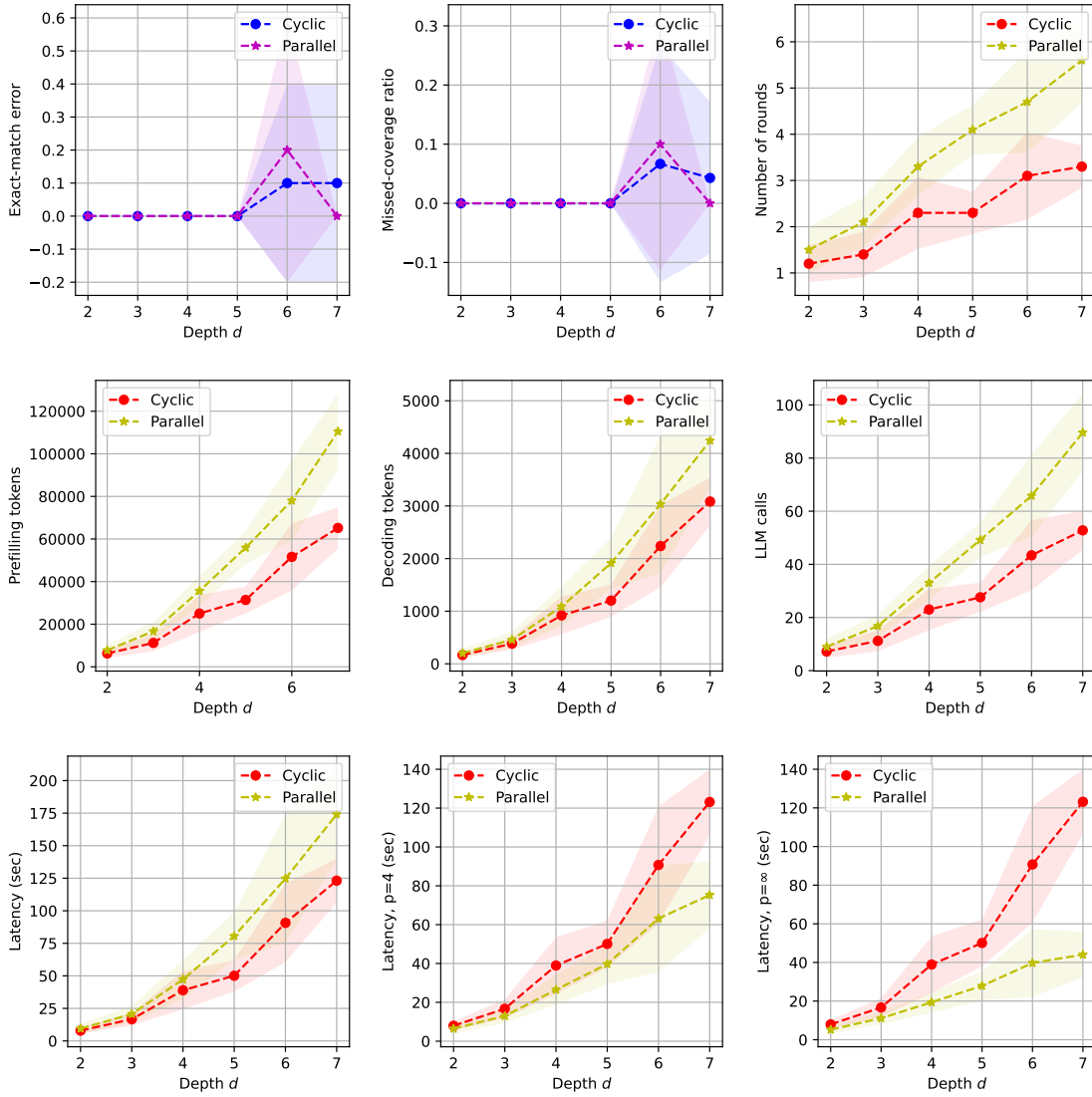


Figure 14: Empirical results (10 trials) for reasoning with iterative retrieval, where two options of retrieval are compared. The degree $g = 1$ and width $w = 100$ are fixed, while the depth d varies. The algorithm uses a chunk size of 100 clues, and prompts the LLM calls responsible for reasoning and answering to think step by step.

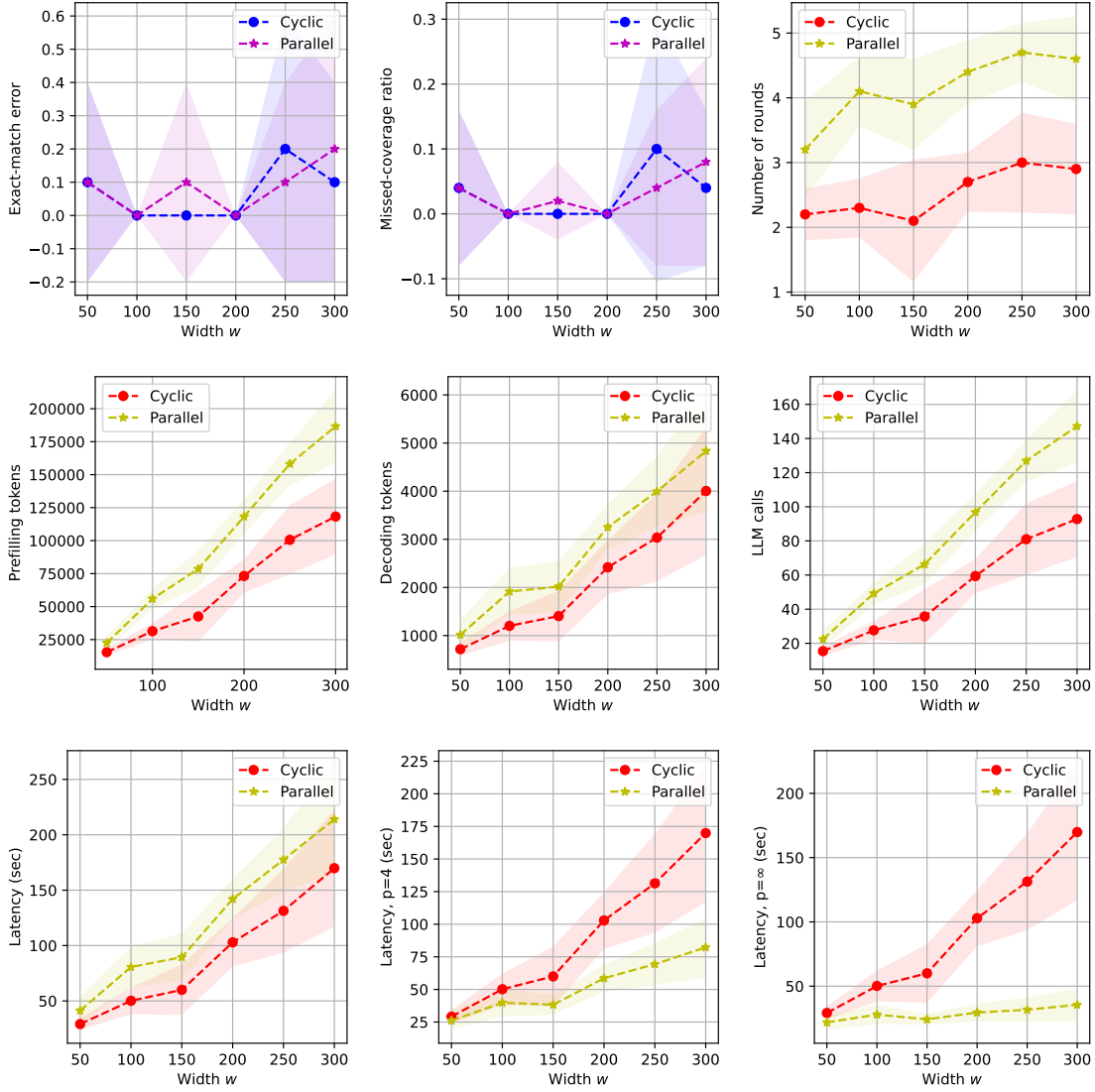


Figure 15: Empirical results (10 trials) for reasoning with iterative retrieval, where two options of retrieval, namely “cyclic” and “parallel”, are compared. The degree $g = 1$ and depth $d = 5$ are fixed, while the width w varies. The algorithm uses a chunk size of 100 clues, and prompts the LLM calls responsible for reasoning and answering to think step by step.

5 Case study: recursive decomposition

This section studies LLM-based algorithms with *recursive task decomposition*, a pattern that is vastly different from those studied in previous sections, and yet still covered by the analytical framework proposed in Section 2. Roughly speaking, a recursive LLM-based algorithm starts from the original task of concern and recursively generates more intermediate sub-tasks, so that each sub-task can be solved by aggregating the solutions to its children tasks, while being unaware of other sub-tasks involved in the overall algorithm. In particular, solving and/or decomposing each sub-task can be achieved by LLM calls, while the outline of recursive task decomposition remains symbolic. Such LLM-based algorithms have been widely applied, e.g. in LAMBADA [KKB⁺23], LLM programs [SSC⁺23], ADaPT [PKH⁺24], THREAD [SMLG24], Recursion of Thought [LK23], Decomposed Prompting [KTF⁺23], ReDel [ZDCB24], among many others.

In the following, we first introduce the concrete task under consideration, and then design a recursive LLM-based algorithm for solving it, highlighting the dynamic construction of its computational graph at runtime. We then provide analysis for its accuracy and efficiency using the proposed framework, which is further validated with numerical experiments; along the way, we derive a formal guarantee for generic LLM-based algorithms, under the technical assumption of additive errors and bounded sensitivity.

5.1 Concrete setup

For concreteness, we consider the same task introduced in Section 4.1 and visualized in Figure 11, which is about calculating a targeted variable based on clues about a grid of many variables.

One major difference here is that we consider much larger depth d , width w and/or degree g for the grid of variables, which implies a larger DAG of needles, i.e. clues relevant to the targeted question. Even if all relevant clues are given *a priori*, the complex reasoning required to answer the targeted question correctly can be well beyond the capability of one single LLM call, which motivates decomposing the reasoning process into multiple LLM calls.

The other major difference is, we assume that the clues are not directly given in plain text, but rather need to be accessed via querying a database. For each query, the database takes a name as input, and returns a clue for the variable of the same name, e.g. “A2 = B1 + B3” for input “A2” or “C1 = 10” for input “C1”. The LLM-based algorithm need to decide by itself what to query from the database. Such a setting is motivated by, and can be regarded as an abstraction of, practical scenarios where an autonomous agent in the wild need to actively retrieve relevant information by itself in order to accomplish a task (unlike in typical problem-solving benchmarks where such information is given), via querying a real database or knowledge graph, using a search engine, retrieving from documents, etc. In this case study, we assume that querying the database does not involve LLM calls, and thus neglect its costs in our analysis.

5.2 Algorithm

We consider the following recursive LLM-based algorithm for solving this task. The overall algorithm maintains a dictionary of variables that have been calculated throughout its execution, and eventually outputs the value returned by applying a function named `ProcessNode` to the targeted variable.

The function `ProcessNode`, which takes the name of a variable as input and returns its numeric value, is defined in a recursive manner:

1. If the input variable is found in the dictionary of calculated variables, then return its value directly.
2. Otherwise, query the database with the input variable, and invoke one LLM call with the returned clue, which is prompted to either answer with a numeric value or conduct further task decomposition, i.e. identifying variables whose values will be necessary and sufficient for calculating the input variable.
 - (a) If the LLM chooses to answer with a numeric value, then return it.
 - (b) Otherwise, invoke `ProcessNode` once for each variable identified by the LLM call, collect the answers returned by these children tasks, and finally invoke one LLM call to calculate and return the numeric value of the input variable.

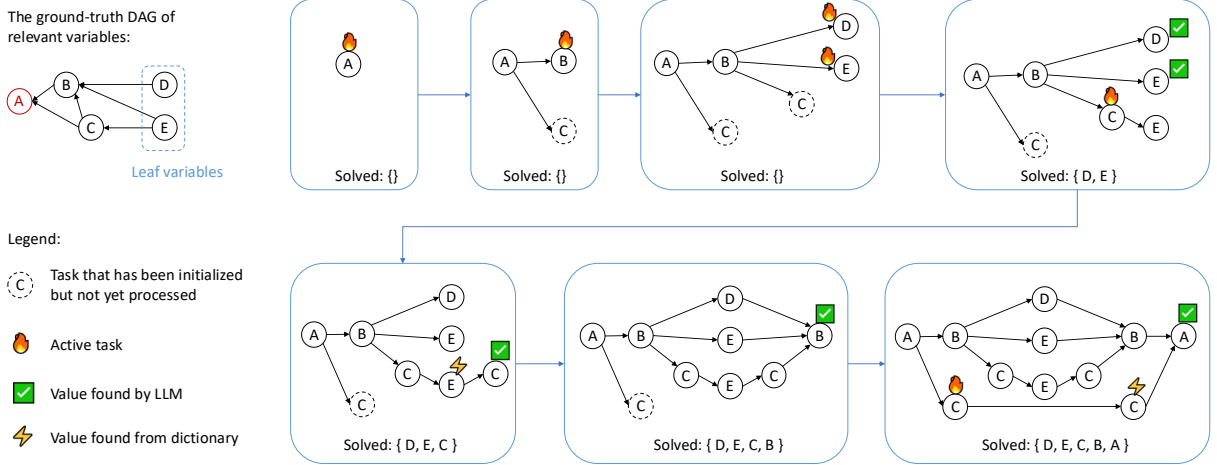


Figure 16: The computational graph of a recursive LLM-based algorithm is constructed dynamically, while a dictionary of solved tasks is maintained (to avoid solving the same intermediate sub-task repetitively) throughout one run of the algorithm.

We make a few comments about this recursive algorithm. (1) The computational graph of this algorithm, or a generic LLM-based algorithm following the pattern of recursive decomposition, is constructed dynamically in a depth-first-search style at runtime. See Figure 16 for a visualization. The final graph is symmetric about the nodes corresponding to the leaf variables (D, E); on the left are LLM calls for identifying children variables for the non-leaf variables (A, B, C), while on the right are LLM calls for calculating their numeric values. (2) The process of complex reasoning is decomposed recursively, so that each LLM call within this algorithm only need to handle a small step of reasoning, whose complexity is irrelevant to that of the overall task. (3) One particular configuration of this algorithm, like in the previous case study, is about how the LLM calls (especially the ones responsible for calculation) are prompted, e.g. to answer directly or think step by step. The impact of this design choice on the accuracy and efficiency of the overall algorithm will be investigated analytically and empirically soon in this section.

5.3 Analysis

5.3.1 Error metrics

Recall from Eq. (1) that for a specific node v with inputs x_1, \dots, x_k , the error of its output y is assumed to be upper bounded by $\mathcal{E}(y) \leq f_v(\mathcal{E}(x_1), \mathcal{E}(x_2), \dots, \mathcal{E}(x_k))$ for some function f_v . For the concrete setting of the current case study, there are two major failure modes for the aforementioned algorithm: errors in recursive task decomposition, and errors in calculating the numeric values of specific variables. Empirical results during our early exploration suggested that LLMs make very few mistakes of the first kind, while the second failure mode is much more common, due to the limited arithmetic capabilities of current LLMs. Moreover, all mathematical operations considered in this concrete settings (including addition, subtraction, maximum and minimum) are 1-Lipschitz continuous with respect to each input variable.

All these motivate us to derive the following error bound, which indeed holds true for any generic LLM-based algorithm represented by a DAG, under the assumption of *additive errors and bounded sensitivity*. The proof is deferred to Section 5.5 after the experiments.

Proposition 2. *Suppose that the assumption of additive errors and bounded sensitivity holds true for an LLM-based algorithm represented by a DAG, namely for each node v with k inputs x_1, \dots, x_k and a single output y , it holds that*

$$\mathcal{E}(y) \leq f_v(\mathcal{E}(x_1), \mathcal{E}(x_2), \dots, \mathcal{E}(x_k)) := \mathcal{E}_v + S \times \sum_{i \in [k]} \mathcal{E}(x_i)$$

for some node-specific additive error \mathcal{E}_v and finite sensitivity parameter $S \geq 0$. Then the error of the output $y(v)$ of any node v , including the one that generates the final output of the overall algorithm, is bounded by

$$\mathcal{E}(y(v)) \leq \sum_{w \in DAG} \sum_{path \in \mathcal{P}(w \rightarrow v)} S^{|path|} \times \mathcal{E}_w. \quad (7)$$

Here, $|path|$ denotes the length of a path on the DAG, while $\mathcal{P}(w \rightarrow v)$ represents the set of paths from node w to node v if $w \neq v$, or a singleton set containing one hypothetical path of length 0 if $w = v$. For the special case of $S = 1$, this upper bound can be simplified as $\mathcal{E}(y(v)) \leq \sum_{w \in DAG} |\mathcal{P}(w \rightarrow v)| \times \mathcal{E}_w$.

This proposition precisely characterizes how the error \mathcal{E}_w of each node w impacts the accuracy of the overall algorithm, via the number and lengths of the paths from each node to the final output.

5.3.2 Cost metrics

Let us first consider the cost of each LLM call. For each leaf variable, one LLM call is needed for finding its numeric value based on its corresponding clue of length $O(1)$, which implies $\mathcal{L}_{pre} \leq \mathcal{L}_{sys} + O(1)$ and $\mathcal{L}_{dec} \leq O(1)$, and thus $\mathcal{C}(\text{leaf}) \leq \mathcal{C}_{LLM}(\mathcal{L}_{sys} + 1, 1)$. For each non-leaf variable, two LLM calls are needed. One of them is responsible for task decomposition, i.e. identifying its g children variables, which implies $\mathcal{L}_{pre} \leq \mathcal{L}_{sys} + O(g)$ and $\mathcal{L}_{dec} \leq O(g)$, and thus $\mathcal{C}(\text{decomposition}) \leq \mathcal{C}_{LLM}(\mathcal{L}_{sys} + g, g)$. The other LLM call is responsible for calculating the numeric value of the current variable based on the values of its children variables, which has $\mathcal{L}_{pre} \leq \mathcal{L}_{sys} + O(g)$, and $\mathcal{L}_{dec} \leq O(1)$ if the LLM is prompted to answer directly, or $\mathcal{L}_{dec} \leq \mathcal{L}_{calc}(g)$ for some function \mathcal{L}_{calc} if it is prompted to do the calculation step by step (e.g. $\mathcal{L}_{calc}(g) \leq O(g)$ or $O(g^2)$, depending on how the LLM executes the calculation with g variables). In sum, we have $\mathcal{C}(\text{calculation}) \leq \mathcal{C}_{LLM}(\mathcal{L}_{sys} + g, 1 \text{ or } \mathcal{L}_{calc}(g))$ for each LLM call responsible for calculation.

The analysis above has also revealed the total number of LLM calls. Let n and n_{leaf} be the number of relevant variables and the number of relevant leaf variables, respectively. These parameters are determined by d, w, g and other factors, as is the case for the ℓ parameter (total length of relevant clues) in Section 4. Recall from above that each leaf variable requires one LLM call for finding its value from its corresponding clue, while each non-leaf variable requires two LLM calls, one for task decomposition and one for calculation. Assuming that task decomposition is done correctly by the LLM for each non-leaf variable, the total number of LLM calls will be $2 \times (n - n_{\text{leaf}}) + n_{\text{leaf}} = 2 \times n - n_{\text{leaf}}$.

Putting things together, we finally arrive at the total cost of the overall recursive algorithm:

$$\mathcal{C} \leq (n - n_{\text{leaf}}) \times \left(\mathcal{C}_{LLM}(\mathcal{L}_{sys} + g, g) + \mathcal{C}_{LLM}(\mathcal{L}_{sys} + g, 1 \text{ or } \mathcal{L}_{calc}(g)) \right) + n_{\text{leaf}} \times \mathcal{C}_{LLM}(\mathcal{L}_{sys}, 1). \quad (8)$$

In particular, prompting the LLM to do the calculation step by step, which is anticipated to significantly improve the accuracy of the overall algorithm, will increase most cost metrics (though not for the number of LLM calls or the total number of prefilling tokens) by a *multiplicative* factor, in contrast to the previous case study in Section 4 where step-by-step prompting incurs a minor *additive* cost.

5.4 Experiments

We validate our analysis via experiments with a `Qwen-2-72B-Instruct` model [YYH+24], supported by vLLM [KLZ+23] and running on a server with 4 Nvidia A100-80G GPUs. For each experiment, we vary the difficulty of the task through the depth d or degree g of the grid of variables, while comparing two options of prompting the LLM calls responsible for calculation, namely “answer directly” and “calculate step by step”.

Empirical results are shown in Figures 17 and 18. For the former, we fix the width $w = 6$ and degree $g = 4$, while varying the depth d ; for the latter, we fix the depth $d = 3$ and width $w = 100$, while varying the degree g . The results confirm our previous analysis: compared to “answer directly”, prompting the LLM calls to “calculate step by step” significantly boosts the accuracy of the overall algorithm and leads to satisfactory performance for a wide range of task configurations, while incurring higher costs in the latency and total number of decoding tokens by a multiplicative factor, and making no difference in the number of LLM calls or total number of prefilling tokens.

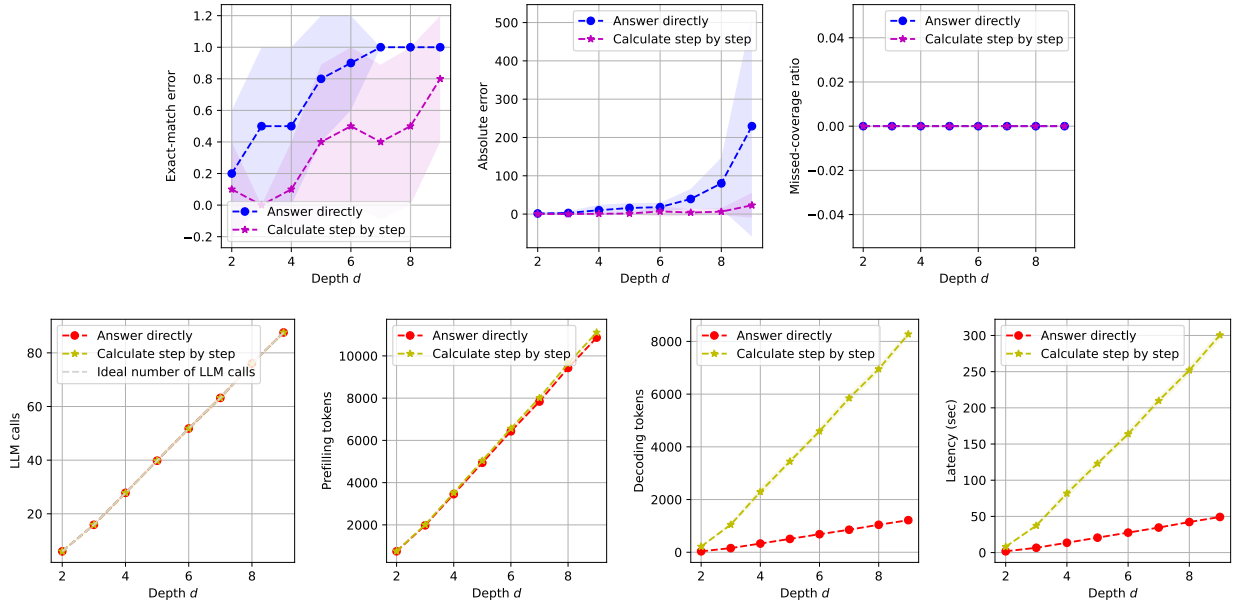


Figure 17: Empirical results (10 trials) for reasoning with recursive task decomposition, where two options of prompting the LLM calls responsible for calculation are compared. The width $w = 6$ and degree $g = 4$ are fixed, while the depth d varies.

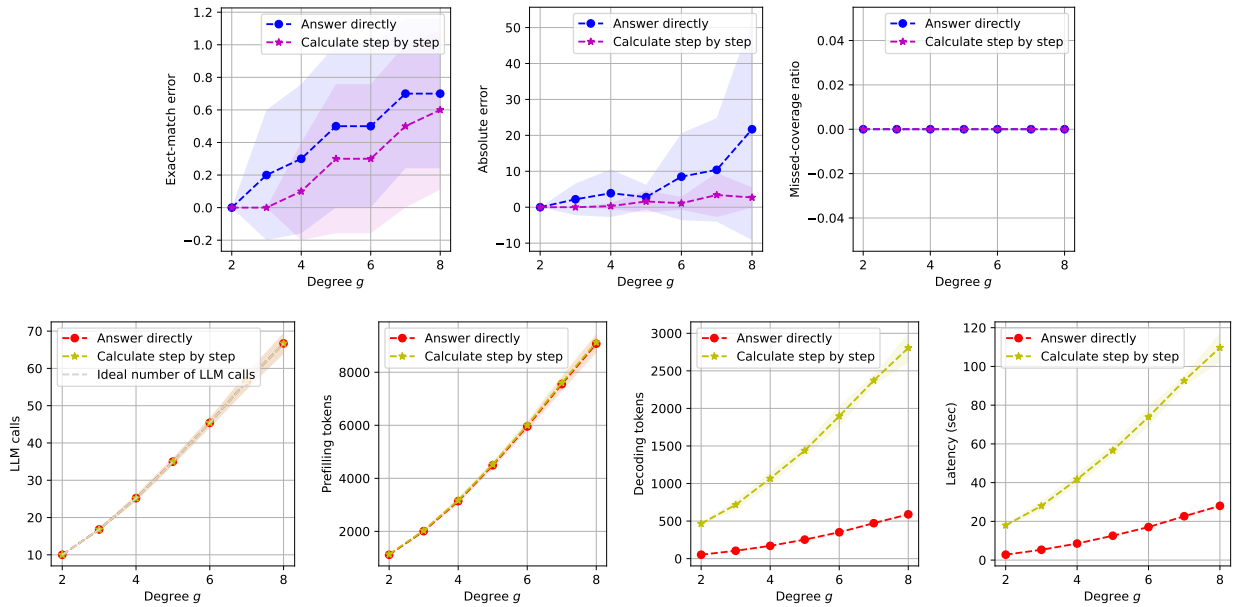


Figure 18: Empirical results (10 trials) for reasoning with recursive task decomposition, where two options of prompting the LLM calls responsible for calculation are compared. The depth $d = 3$ and width $w = 100$ are fixed, while the degree g varies.

5.5 Proof of Proposition 2

We prove the proposition by induction. First, consider the base case where v is a leaf node of the DAG that has no input. Then it can be checked that Eq. (7) holds true:

$$\mathcal{E}(y(v)) \leq \mathcal{E}_v = \sum_{w \in \text{DAG}} \sum_{\text{path} \in \mathcal{P}(w \rightarrow v)} S^{|\text{path}|} \times \mathcal{E}_w.$$

The inequality follows the assumption, while the equality holds true because $\mathcal{P}(w \rightarrow v)$ for a leaf node v is an empty set unless $w = v$, in which case $\mathcal{P}(w \rightarrow v)$ contains only a hypothetical path of length 0.

Next, consider a non-leaf node v , whose predecessor nodes are denoted by u_1, u_2, \dots, u_k . Suppose that Eq. (7) holds true for each u_i , namely

$$\mathcal{E}(y(u_i)) \leq \sum_{w \in \text{DAG}} \sum_{\text{path} \in \mathcal{P}(w \rightarrow u_i)} S^{|\text{path}|} \times \mathcal{E}_w, \quad i \in [k].$$

To prove that Eq. (7) also holds true for node v , we start with the following:

$$\begin{aligned} \mathcal{E}(y(v)) &\leq \mathcal{E}_v + S \times \sum_{i \in [k]} \mathcal{E}(y(u_i)) \\ &\leq \mathcal{E}_v + S \times \sum_{i \in [k]} \sum_{w \in \text{DAG}} \sum_{\text{path} \in \mathcal{P}(w \rightarrow u_i)} S^{|\text{path}|} \times \mathcal{E}_w \\ &= \mathcal{E}_v + S \times \sum_{i \in [k]} \sum_{w \in \text{DAG} \setminus \{v\}} \sum_{\text{path} \in \mathcal{P}(w \rightarrow u_i)} S^{|\text{path}|} \times \mathcal{E}_w \\ &= \mathcal{E}_v + S \times \sum_{w \in \text{DAG} \setminus \{v\}} \sum_{i \in [k]} \sum_{\text{path} \in \mathcal{P}(w \rightarrow u_i)} S^{|\text{path}|} \times \mathcal{E}_w \\ &= \mathcal{E}_v + \sum_{w \in \text{DAG} \setminus \{v\}} \sum_{i \in [k]} \sum_{\text{path} \in \mathcal{P}(w \rightarrow u_i)} S^{|\text{path}|+1} \times \mathcal{E}_w. \end{aligned}$$

Here in the third line, we replace the summation over $w \in \text{DAG}$ with $w \in \text{DAG} \setminus \{v\}$, since there is certainly no path from node v to its predecessor node u_i . To move forward, notice that $\mathcal{P}(w \rightarrow v)$ is a union of k disjoint sets, where the i -th set contains paths ending with the directed edge from u_i to v :

$$\mathcal{P}(w \rightarrow v) = \bigcup_{i \in [k]} \left\{ \text{path} + [u_i \rightarrow v] : \text{path} \in \mathcal{P}(w \rightarrow u_i) \right\}.$$

With this, we can further simplify the previous upper bound:

$$\begin{aligned} \mathcal{E}(y(v)) &\leq \mathcal{E}_v + \sum_{w \in \text{DAG} \setminus \{v\}} \sum_{i \in [k]} \sum_{\text{path} \in \mathcal{P}(w \rightarrow u_i)} S^{|\text{path}|+1} \times \mathcal{E}_w \\ &= \mathcal{E}_v + \sum_{w \in \text{DAG} \setminus \{v\}} \sum_{\text{path} \in \mathcal{P}(w \rightarrow v)} S^{|\text{path}|} \times \mathcal{E}_w \\ &= \sum_{w \in \text{DAG}} \sum_{\text{path} \in \mathcal{P}(w \rightarrow v)} S^{|\text{path}|} \times \mathcal{E}_w. \end{aligned}$$

This concludes our proof of the proposition.

6 Related works

LLM-based algorithms. The concept of LLM-based algorithms, as was explained in Section 1, is fairly broad and general, ranging from a combination of one or multiple LLM calls with some prompt engineering [YYZ⁺23, BBK⁺23, BMZ⁺24, LLLD23, SLC⁺23, ZSH⁺23, WWS⁺23, PKH⁺24, CLGI24], to LLM-powered agent systems [MDL⁺23, WBZ⁺23, HZC⁺24, GLP⁺24, SST⁺23, ZWK⁺24, PKB⁺24, XCG⁺23, QXW⁺24, KSS⁺24] and compound AI systems [ZKC⁺24, CDH⁺24] that augment LLMs with additional abilities like tool use and long-term memory, and to the emerging paradigm of LLM programming [SSC⁺23, KTF⁺23, KSM⁺24, ZYX⁺24, KVG⁺24]. Some elements of our analytical framework proposed in Section 2, such as the principle of task decomposition, the computational-graph representation, evaluation of and comparison between LLM-based algorithms with accuracy and efficiency taken into account simultaneously, etc., have already appeared in one way or another in these prior works. It is primarily our *unified, systematic and formal* investigation into the design and analysis of *generic* LLM-based algorithms that distinguishes the current work from this vast literature.

Scaling properties of LLM test-time computation. Recent works have started to investigate, analytically or empirically, the scaling properties of LLM test-time computation.

One line of research is concerned about the scaling properties of repeated sampling, e.g. randomly sampling multiple generations for the same prompt and then aggregating the results [CDH⁺24, BJE⁺24, SLXK24, WSL⁺24], which might be regarded as a stochastic version of parallel decomposition investigated in Section 3. Our work is orthogonal and complementary to this line of research, as our analysis is deterministic and targeted at generic patterns of LLM-based algorithms. Indeed, one potential direction for expanding the analytical framework proposed in this work would be to augment it with stochastic decoding and repeated sampling, along with relevant theoretical results from prior works.

Another line of works is concerned about improving the output quality of an LLM call, albeit at a higher cost, by generating more tokens autoregressively, e.g. via chains of thoughts [WWS⁺22] or step-by-step reasoning [KGR⁺22]. This idea has been investigated theoretically [FZG⁺23, MS24, LLZM24], and further popularized recently by the OpenAI o1 model [Ope24c]. As this approach of scaling up the test-time computation of *individual* LLM calls is becoming more widely adopted, it is important to understand, analytically and quantitatively, how it will impact the *overall* accuracy and efficiency when such LLM calls are embedded within an LLM-based algorithm. Our work can be useful in achieving this, as illustrated in the case studies in Sections 4 and 5, where the impacts of prompting LLM calls to “think step by step” versus “answer directly” can be characterized analytically with our proposed framework.

Learning-augmented algorithms. Our work draws inspiration from the research area of algorithms with predictions / learning-augmented algorithms [MV22, LM22]. One standard paradigm of this area is to consider a specific task (say sorting [BC23] or clustering [EFS⁺22]), assume access to a black-box machine learning model that satisfies certain properties (e.g. what additional computation or information it can offer), propose a novel algorithm that leverages this ML model, provide theoretical guarantees for its accuracy and efficiency, and show the improvements over traditional, purely symbolic algorithms. Our work is similar in spirit to this line of research, but also substantially different, in that our analytical framework is targeted at general tasks and LLM-based algorithms, with assumptions on the capabilities, limitations and inference service of LLMs (regarded as general-purpose problem solvers) that are quite different from typical assumptions for task-specific ML models in the literature of learning-augmented algorithms.

7 Conclusion and discussion

We have introduced a formal framework for studying the design and analysis of LLM-based algorithms. After identifying the computational-graph representation, the principle of task decomposition, and other abstractions, we find it feasible to provide formal analysis for the accuracy and efficiency of generic LLM-based algorithms. In multiple case studies, we provide in-depth analysis with numerical validation for various patterns of LLM-based algorithms, including parallel, hierarchical and recursive decomposition.

Moving forward, we find it promising future research to further expand or apply the proposed framework and thereby advance the field of LLM-based algorithms, from a theoretical or practical perspective. For example:

- We have been assuming that LLM nodes are state-less, and only considering the simplest and most straightforward usage of LLMs, i.e. sending a prompt and receiving a response for each LLM call. One potential extension is to consider LLM nodes with states, like short-term memory in agent systems, or other advanced ways of using LLMs, and understand how accuracy and efficiency of LLM-based algorithms are impacted in such cases.
- In our empirical study, we have mainly focused on the hyperparameter m that indicates the granularity of parallel task decomposition, or the option of prompting certain LLM calls to either answer directly or think step by step. Future work might place more emphasis on other configurations of LLM-based algorithms, such as the choices of LLM models (e.g. choosing a strong-but-expensive model for specific LLM calls and a weak-but-cheap one for the others within the same algorithm), LLM decoding methods (e.g. greedy vs. stochastic [WWS⁺23, CDH⁺24, BJE⁺24]), etc., and better understand how they impact the accuracy and efficiency of LLM-based algorithms.
- Through our abstractions of multiple error and cost metrics for the same task, we have touched upon the topics of multi-objective optimization and hyperparameter optimization. Future work might try to formally investigate these aspects.
- From a more practical perspective, future work might adopt the proposed framework, or some components and methodology within it, to assist the design, analysis, improvement and application of new LLM-based algorithms, or for fair comparison between different algorithms, with both accuracy and efficiency taken into account.

Given the plenty of opportunities for future research on LLM-based algorithms, we would like to invite the community to contribute to this exciting and rapidly developing field, using the current work as a starting point.

Acknowledgements

The authors would like to thank Yuchang Sun for helpful discussion, as well as the AgentScope team, especially Xuchen Pan, Dawei Gao and Weirui Kuang, for their assistance with using AgentScope and setting up LLM inference service for the experiments.

References

- [AQS⁺23] M. Agarwal, A. Qureshi, N. Sardana, L. Li, J. Quevedo, and D. Khudia. LLM Inference Performance Engineering: Best Practices. <https://www.databricks.com/blog/llm-inference-performance-engineering-best-practices>, 2023.
- [BBK⁺23] M. Besta, N. Blach, A. Kubíček, R. Gerstenberger, L. Gianinazzi, J. Gajda, T. Lehmann, M. Podstawski, H. Niewiadomski, P. Nyczyk, and T. Hoefler. Graph of Thoughts: Solving Elaborate Problems with Large Language Models. In *AAAI Conference on Artificial Intelligence*, 2023.
- [BC23] X. Bai and C. Coester. Sorting with Predictions. In *Thirty-seventh Conference on Neural Information Processing Systems*, 2023.
- [BCE⁺23] S. Bubeck, V. Chandrasekaran, R. Eldan, J. Gehrke, E. Horvitz, E. Kamar, P. Lee, Y. T. Lee, Y. Li, S. Lundberg, H. Nori, H. Palangi, M. T. Ribeiro, and Y. Zhang. Sparks of Artificial General Intelligence: Early experiments with GPT-4. *arXiv*, 2023.
- [BJE⁺24] B. Brown, J. Juravsky, R. Ehrlich, R. Clark, Q. V. Le, C. Ré, and A. Mirhoseini. Large Language Monkeys: Scaling Inference Compute with Repeated Sampling. *arXiv*, 2024.
- [BMZ⁺24] M. Besta, F. Memedi, Z. Zhang, R. Gerstenberger, G. Piao, N. Blach, P. Nyczyk, M. Copik, G. Kwasniewski, J. Muller, L. Gianinazzi, A. Kubíček, H. Niewiadomski, A. O’Mahony, O. Mutlu, and T. Hoefler. Demystifying Chains, Trees, and Graphs of Thoughts. *arXiv*, 2024.
- [CDH⁺24] L. Chen, J. Q. Davis, B. Hanin, P. Bailis, I. Stoica, M. Zaharia, and J. Zou. Are More LLM Calls All You Need? Towards Scaling Laws of Compound Inference Systems. *arXiv*, 2024.
- [CEP⁺21] S. Chaudhuri, K. Ellis, O. Polozov, R. Singh, A. Solar-Lezama, and Y. Yue. Neurosymbolic Programming. *Foundations and Trends in Programming Languages*, 7(3):158–243, 2021.
- [CLGI24] Y. Chang, K. Lo, T. Goyal, and M. Iyyer. BoookScore: A systematic exploration of book-length summarization in the era of LLMs. In *The Twelfth International Conference on Learning Representations*, 2024.
- [CSH23] A. Creswell, M. Shanahan, and I. Higgins. Selection-Inference: Exploiting Large Language Models for Interpretable Logical Reasoning. In *The Eleventh International Conference on Learning Representations*, 2023.
- [DG08] J. Dean and S. Ghemawat. MapReduce: simplified data processing on large clusters. *Communications of the ACM*, 51:107–113, 2008.
- [EFS⁺22] J. C. Ergun, Z. Feng, S. Silwal, D. Woodruff, and S. Zhou. Learning-Augmented k-means Clustering. In *International Conference on Learning Representations*, 2022.
- [FZG⁺23] G. Feng, B. Zhang, Y. Gu, H. Ye, D. He, and L. Wang. Towards Revealing the Mystery behind Chain of Thought: A Theoretical Perspective. In *Thirty-seventh Conference on Neural Information Processing Systems*, 2023.
- [GK23] T. Gupta and A. Kembhavi. Visual Programming: Compositional visual reasoning without training. In *Proceedings of the IEEE Computer Society Conference on Computer Vision and Pattern Recognition*, volume 2023-June, pages 14953–14962, 2023.
- [GLP⁺24] D. Gao, Z. Li, X. Pan, W. Kuang, Z. Ma, B. Qian, F. Wei, W. Zhang, Y. Xie, D. Chen, L. Yao, H. Peng, Z. Zhang, L. Zhu, C. Cheng, H. Shi, Y. Li, B. Ding, and J. Zhou. AgentScope: A Flexible yet Robust Multi-Agent Platform. *arXiv*, 2024.
- [GXG⁺24] Y. Gao, Y. Xiong, X. Gao, K. Jia, J. Pan, Y. Bi, Y. Dai, J. Sun, M. Wang, and H. Wang. Retrieval-Augmented Generation for Large Language Models: A Survey. *arXiv*, 2024.

- [HR24] M. Hahn and M. Rofin. Why are Sensitive Functions Hard for Transformers? *arXiv*, 2024.
- [HZC⁺24] S. Hong, M. Zhuge, J. Chen, X. Zheng, Y. Cheng, J. Wang, C. Zhang, Z. Wang, S. K. S. Yau, Z. Lin, L. Zhou, C. Ran, L. Xiao, C. Wu, and J. Schmidhuber. MetaGPT: Meta Programming for A Multi-Agent Collaborative Framework. In *The Twelfth International Conference on Learning Representations*, 2024.
- [Kam23] G. Kamradt. LLMTest-NeedleInAHaystack. https://github.com/gkamradt/LLMTest_NeedleInAHaystack, 2023.
- [KBA⁺24] Y. Kuratov, A. Bulatov, P. Anokhin, D. Sorokin, A. Sorokin, and M. Burtsev. In Search of Needles in a 11M Haystack: Recurrent Memory Finds What LLMs Miss. *arXiv*, 2024.
- [KGR⁺22] T. Kojima, S. S. Gu, M. Reid, Y. Matsuo, and Y. Iwasawa. Large Language Models are Zero-Shot Reasoners. In *Advances in Neural Information Processing Systems*, volume 35, pages 22199–22213, 2022.
- [KKB⁺23] M. Kazemi, N. Kim, D. Bhatia, X. Xu, and D. Ramachandran. LAMBADA: Backward Chaining for Automated Reasoning in Natural Language. In *Proceedings of the 61st Annual Meeting of the Association for Computational Linguistics (Volume 1: Long Papers)*, pages 6547–6568, 2023.
- [KLZ⁺23] W. Kwon, Z. Li, S. Zhuang, Y. Sheng, L. Zheng, C. H. Yu, J. E. Gonzalez, H. Zhang, and I. Stoica. Efficient Memory Management for Large Language Model Serving with PagedAttention. In *Proceedings of the ACM SIGOPS 29th Symposium on Operating Systems Principles*, 2023.
- [KRA⁺22] W. Kryscinski, N. Rajani, D. Agarwal, C. Xiong, and D. Radev. BOOKSUM: A Collection of Datasets for Long-form Narrative Summarization. In *Findings of the Association for Computational Linguistics: EMNLP 2022*, pages 6536–6558, 2022.
- [KSM⁺24] O. Khattab, A. Singhvi, P. Maheshwari, Z. Zhang, K. Santhanam, S. V. A, S. Haq, A. Sharma, T. T. Joshi, H. Moazam, H. Miller, M. Zaharia, and C. Potts. DSPy: Compiling Declarative Language Model Calls into State-of-the-Art Pipelines. In *The Twelfth International Conference on Learning Representations*, 2024.
- [KSS⁺24] S. Kapoor, B. Stroebel, Z. S. Siegel, N. Nadgir, and A. Narayanan. AI Agents That Matter. *arXiv*, 2024.
- [KTF⁺23] T. Khot, H. Trivedi, M. Finlayson, Y. Fu, K. Richardson, P. Clark, and A. Sabharwal. Decomposed Prompting: A Modular Approach for Solving Complex Tasks. In *The Eleventh International Conference on Learning Representations*, 2023.
- [KVG⁺24] S. Kambhampati, K. Valmeekam, L. Guan, M. Verma, K. Stechly, S. Bhambri, L. P. Saldyt, and A. B. Murthy. Position: LLMs can’t plan, but can help planning in llm-modulo frameworks. In *Forty-first International Conference on Machine Learning*, 2024.
- [LFXW24] P. Laban, A. R. Fabbri, C. Xiong, and C.-S. Wu. Summary of a Haystack: A Challenge to Long-Context LLMs and RAG Systems. *arXiv*, 2024.
- [LK23] S. Lee and G. Kim. Recursion of Thought: A Divide-and-Conquer Approach to Multi-Context Reasoning with Language Models. In A. Rogers, J. Boyd-Graber, and N. Okazaki, editors, *Findings of the Association for Computational Linguistics: ACL 2023*, pages 623–658, 2023.
- [LLLD23] B. Lei, P.-H. Lin, C. Liao, and C. Ding. Boosting Logical Reasoning in Large Language Models through a New Framework: The Graph of Thought. *arXiv*, 2023.
- [LLZM24] Z. Li, H. Liu, D. Zhou, and T. Ma. Chain of Thought Empowers Transformers to Solve Inherently Serial Problems. In *The Twelfth International Conference on Learning Representations*, 2024.
- [LM22] A. Lindermayr and N. Megow. Algorithms with Predictions. <https://algorithms-with-predictions.github.io>, 2022.

- [LPP⁺20] P. Lewis, E. Perez, A. Piktus, F. Petroni, V. Karpukhin, N. Goyal, H. Küttler, M. Lewis, W.-t. Yih, T. Rocktäschel, S. Riedel, and D. Kiela. Retrieval-augmented generation for knowledge-intensive NLP tasks. In *Proceedings of the 34th International Conference on Neural Information Processing Systems*, 2020.
- [LZLC24] M. Li, S. Zhang, Y. Liu, and K. Chen. NeedleBench: Can LLMs Do Retrieval and Reasoning in 1 Million Context Window? *arXiv*, 2024.
- [MDL⁺23] G. Mialon, R. Dessi, M. Lomeli, C. Nalmpantis, R. Pasunuru, R. Raileanu, B. Roziere, T. Schick, J. Dwivedi-Yu, A. Celikyilmaz, E. Grave, Y. LeCun, and T. Scialom. Augmented Language Models: a Survey. *Transactions on Machine Learning Research*, 2023.
- [Met24] Meta. Meta Llama 3. <https://ai.meta.com/blog/meta-llama-3>, 2024.
- [MJ23] A. Mohtashami and M. Jaggi. Random-access infinite context length for transformers. In *Advances in Neural Information Processing Systems*, 2023.
- [MPS24] W. Merrill, J. Petty, and A. Sabharwal. The Illusion of State in State-Space Models. *arXiv*, 2024.
- [MS23] W. Merrill and A. Sabharwal. The Parallelism Tradeoff: Limitations of Log-Precision Transformers. *Transactions of the Association for Computational Linguistics*, 11:531–545, 2023.
- [MS24] W. Merrill and A. Sabharwal. The Expressive Power of Transformers with Chain of Thought. In *The Twelfth International Conference on Learning Representations*, 2024.
- [MV22] M. Mitzenmacher and S. Vassilvitskii. Algorithms with Predictions. *Communications of the ACM*, 65(7):33–35, 2022.
- [oll23] ollama. ollama. <https://github.com/ollama/ollama>, 2023.
- [Ope24a] OpenAI. GPT-4 Technical Report. *arXiv*, 2024.
- [Ope24b] OpenAI. OpenAI Cookbook: Summarizing Long Documents. https://cookbook.openai.com/examples/summarizing_long_documents, 2024.
- [Ope24c] OpenAI. OpenAI o1 System Card. <https://openai.com/index/openai-o1-system-card/>, 2024.
- [PDC⁺23] R. Pope, S. Douglas, A. Chowdhery, J. Devlin, J. Bradbury, J. Heek, K. Xiao, S. Agrawal, and J. Dean. Efficiently Scaling Transformer Inference. In *Proceedings of Machine Learning and Systems*, volume 5, pages 606–624, 2023.
- [PKB⁺24] P. Pezeshkpour, E. Kandogan, N. Bhutani, S. Rahman, T. Mitchell, and E. Hruschka. Reasoning Capacity in Multi-Agent Systems: Limitations, Challenges and Human-Centered Solutions. *arXiv*, 2024.
- [PKH⁺24] A. Prasad, A. Koller, M. Hartmann, P. Clark, A. Sabharwal, M. Bansal, and T. Khot. ADaPT: As-needed decomposition and planning with language models. In K. Duh, H. Gomez, and S. Bethard, editors, *Findings of the Association for Computational Linguistics: NAACL 2024*, pages 4226–4252. Association for Computational Linguistics, 2024.
- [PNP24] B. Peng, S. Narayanan, and C. Papadimitriou. On Limitations of the Transformer Architecture. *arXiv*, 2024.
- [QT24] Qwen-Team. Generalizing an LLM from 8k to 1M Context using Qwen-Agent, May 2024.
- [QXW⁺24] C. Qian, Z. Xie, Y. Wang, W. Liu, Y. Dang, Z. Du, W. Chen, C. Yang, Z. Liu, and M. Sun. Scaling Large-Language-Model-based Multi-Agent Collaboration. *arXiv*, 2024.

- [Rou23] A. Roucher. LongContext-vs-RAG-NeedleInAHaystack. https://github.com/aymeric-roucher/LongContext_vs_RAG_NeedleInAHaystack, 2023.
- [SCM⁺23] F. Shi, X. Chen, K. Misra, N. Scales, D. Dohan, E. Chi, N. Schärli, and D. Zhou. Large language models can be easily distracted by irrelevant context. In *Proceedings of the 40th International Conference on Machine Learning*, 2023.
- [SLC⁺23] S. Saha, O. Levy, A. Celikyilmaz, M. Bansal, J. Weston, and X. Li. Branch-Solve-Merge Improves Large Language Model Evaluation and Generation. *arXiv*, 2023.
- [SLXK24] C. Snell, J. Lee, K. Xu, and A. Kumar. Scaling LLM Test-Time Compute Optimally can be More Effective than Scaling Model Parameters. *arXiv*, 2024.
- [SMK23] R. Schaeffer, B. Miranda, and S. Koyejo. Are Emergent Abilities of Large Language Models a Mirage? In *Thirty-seventh Conference on Neural Information Processing Systems*, 2023.
- [SMLG24] P. Schroeder, N. Morgan, H. Luo, and J. Glass. THREAD: Thinking Deeper with Recursive Spawning. *arXiv*, 2024.
- [SSC⁺23] I. Schlag, S. Sukhbaatar, A. Celikyilmaz, W.-t. Yih, J. Weston, J. Schmidhuber, and X. Li. Large Language Model Programs. *arXiv*, 2023.
- [SST⁺23] Y. Shen, K. Song, X. Tan, D. Li, W. Lu, and Y. Zhuang. HuggingGPT: Solving AI Tasks with ChatGPT and its Friends in Hugging Face. *arXiv*, 2023.
- [TTC⁺24] J. Thomm, A. Terzic, G. Camposampiero, M. Hersche, B. Schölkopf, and A. Rahimi. Limits of Transformer Language Models on Learning to Compose Algorithms. *arXiv*, 2024.
- [VFK⁺22] J. Vig, A. Fabbri, W. Kryscinski, C.-S. Wu, and W. Liu. Exploring Neural Models for Query-Focused Summarization. In *Findings of the Association for Computational Linguistics: NAACL 2022*, pages 1455–1468, 2022.
- [VSP⁺17] A. Vaswani, N. Shazeer, N. Parmar, J. Uszkoreit, L. Jones, A. N. Gomez, Ł. Kaiser, and I. Polosukhin. Attention is All you Need. In *Advances in Neural Information Processing Systems*, volume 30, 2017.
- [WBC⁺15] J. Weston, A. Bordes, S. Chopra, A. M. Rush, B. van Merriënboer, A. Joulin, and T. Mikolov. Towards AI-Complete Question Answering: A Set of Prerequisite Toy Tasks. *arXiv*, 2015.
- [WBZ⁺23] Q. Wu, G. Bansal, J. Zhang, Y. Wu, B. Li, E. Zhu, L. Jiang, X. Zhang, S. Zhang, J. Liu, A. H. Awadallah, R. W. White, D. Burger, and C. Wang. AutoGen: Enabling Next-Gen LLM Applications via Multi-Agent Conversation Framework. *arXiv*, 2023.
- [WDL24] K. Wen, X. Dang, and K. Lyu. RNNs are not Transformers (Yet): The Key Bottleneck on In-context Retrieval. *arXiv*, 2024.
- [WOZ⁺21] J. Wu, L. Ouyang, D. M. Ziegler, N. Stiennon, R. Lowe, J. Leike, and P. Christiano. Recursively Summarizing Books with Human Feedback. *arXiv*, 2021.
- [WSL⁺24] Y. Wu, Z. Sun, S. Li, S. Welleck, and Y. Yang. An Empirical Analysis of Compute-Optimal Inference for Problem-Solving with Language Models. *arXiv*, 2024.
- [WTB⁺22] J. Wei, Y. Tay, R. Bommasani, C. Raffel, B. Zoph, S. Borgeaud, D. Yogatama, M. Bosma, D. Zhou, D. Metzler, E. H. Chi, T. Hashimoto, O. Vinyals, P. Liang, J. Dean, and W. Fedus. Emergent Abilities of Large Language Models. *Transactions on Machine Learning Research*, 2022.
- [WWS⁺22] J. Wei, X. Wang, D. Schuurmans, M. Bosma, E. H. hsin Chi, F. Xia, Q. Le, and D. Zhou. Chain of Thought Prompting Elicits Reasoning in Large Language Models. In *Advances in Neural Information Processing Systems*, 2022.

- [WWS⁺23] X. Wang, J. Wei, D. Schuurmans, Q. V. Le, E. H. Chi, S. Narang, A. Chowdhery, and D. Zhou. Self-Consistency Improves Chain of Thought Reasoning in Language Models. In *The Eleventh International Conference on Learning Representations*, 2023.
- [XCG⁺23] Z. Xi, W. Chen, X. Guo, W. He, Y. Ding, B. Hong, M. Zhang, J. Wang, S. Jin, E. Zhou, R. Zheng, X. Fan, X. Wang, L. Xiong, Y. Zhou, W. Wang, C. Jiang, Y. Zou, X. Liu, Z. Yin, S. Dou, R. Weng, W. Cheng, Q. Zhang, W. Qin, Y. Zheng, X. Qiu, X. Huang, and T. Gui. The Rise and Potential of Large Language Model Based Agents: A Survey. *arXiv*, 2023.
- [XJW⁺24] G. Xiong, Q. Jin, X. Wang, M. Zhang, Z. Lu, and A. Zhang. Improving Retrieval-Augmented Generation in Medicine with Iterative Follow-up Questions. *arXiv*, 2024.
- [YQZ⁺18] Z. Yang, P. Qi, S. Zhang, Y. Bengio, W. Cohen, R. Salakhutdinov, and C. D. Manning. HotpotQA: A Dataset for Diverse, Explainable Multi-hop Question Answering. In *Proceedings of the 2018 Conference on Empirical Methods in Natural Language Processing*, pages 2369–2380, 2018.
- [YSZ⁺24] Z. Yuan, Y. Shang, Y. Zhou, Z. Dong, Z. Zhou, C. Xue, B. Wu, Z. Li, Q. Gu, Y. J. Lee, Y. Yan, B. Chen, G. Sun, and K. Keutzer. LLM Inference Unveiled: Survey and Roofline Model Insights. *arXiv*, 2024.
- [YXLAZ24] T. Ye, Z. Xu, Y. Li, and Z. Allen-Zhu. Physics of Language Models: Part 2.1, Grade-School Math and the Hidden Reasoning Process. *arXiv*, 2024.
- [YYH⁺24] A. Yang, B. Yang, B. Hui, B. Zheng, B. Yu, C. Zhou, C. Li, C. Li, D. Liu, F. Huang, G. Dong, H. Wei, H. Lin, J. Tang, J. Wang, J. Yang, J. Tu, J. Zhang, J. Ma, J. Yang, J. Xu, J. Zhou, J. Bai, J. He, J. Lin, K. Dang, K. Lu, K. Chen, K. Yang, M. Li, M. Xue, N. Ni, P. Zhang, P. Wang, R. Peng, R. Men, R. Gao, R. Lin, S. Wang, S. Bai, S. Tan, T. Zhu, T. Li, T. Liu, W. Ge, X. Deng, X. Zhou, X. Ren, X. Zhang, X. Wei, X. Ren, X. Liu, Y. Fan, Y. Yao, Y. Zhang, Y. Wan, Y. Chu, Y. Liu, Z. Cui, Z. Zhang, Z. Guo, and Z. Fan. Qwen2 Technical Report. *arXiv*, 2024.
- [YYZ⁺23] S. Yao, D. Yu, J. Zhao, I. Shafran, T. L. Griffiths, Y. Cao, and K. R. Narasimhan. Tree of Thoughts: Deliberate Problem Solving with Large Language Models. In *Thirty-seventh Conference on Neural Information Processing Systems*, 2023.
- [YZY⁺23] S. Yao, J. Zhao, D. Yu, N. Du, I. Shafran, K. Narasimhan, and Y. Cao. ReAct: Synergizing Reasoning and Acting in Language Models. In *The Eleventh International Conference on Learning Representations*, 2023.
- [ZCH⁺24] X. Zhang, Y. Chen, S. Hu, Z. Xu, J. Chen, M. K. Hao, X. Han, Z. L. Thai, S. Wang, Z. Liu, and M. Sun. ∞ Bench: Extending Long Context Evaluation Beyond 100K Tokens. *arXiv*, 2024.
- [ZDCB24] A. Zhu, L. Dugan, and C. Callison-Burch. ReDel: A Toolkit for LLM-Powered Recursive Multi-Agent Systems. *arXiv*, 2024.
- [ZKC⁺24] M. Zaharia, O. Khattab, L. Chen, J. Q. Davis, H. Miller, C. Potts, J. Zou, M. Carbin, J. Frankle, N. Rao, and A. Ghodsi. The Shift from Models to Compound AI Systems. <https://bair.berkeley.edu/blog/2024/02/18/compound-ai-systems>, 2024.
- [ZNH⁺24] Z. Zhou, X. Ning, K. Hong, T. Fu, J. Xu, S. Li, Y. Lou, L. Wang, Z. Yuan, X. Li, S. Yan, G. Dai, X.-P. Zhang, Y. Dong, and Y. Wang. A Survey on Efficient Inference for Large Language Models. *arXiv*, 2024.
- [ZSH⁺23] D. Zhou, N. Schärli, L. Hou, J. Wei, N. Scales, X. Wang, D. Schuurmans, C. Cui, O. Bousquet, Q. V. Le, and E. H. Chi. Least-to-Most Prompting Enables Complex Reasoning in Large Language Models. In *The Eleventh International Conference on Learning Representations*, 2023.

- [ZWK⁺24] M. Zhuge, W. Wang, L. Kirsch, F. Faccio, D. Khizbullin, and J. Schmidhuber. GPTSwarm: Language Agents as Optimizable Graphs. In *Forty-first International Conference on Machine Learning*, 2024.
- [ZYY⁺24] L. Zheng, L. Yin, Z. Xie, C. Sun, J. Huang, C. H. Yu, S. Cao, C. Kozyrakis, I. Stoica, J. E. Gonzalez, C. Barrett, and Y. Sheng. SGLang: Efficient Execution of Structured Language Model Programs. *arXiv*, 2024.
- [ZYY24] Y. Zhang, Y. Yuan, and A. C.-C. Yao. Meta Prompting for AI Systems. *arXiv*, 2024.